THE EFFECT OF CALCIUM ADDITION ON THE DISSOLUTION OF HYDROXYAPATITE

by

Wenfu Wang

Bachelor of Science, Physics, Nanjing University, 2013

Submitted to the Graduate Faculty of

Swanson School of Engineering in partial fulfillment

of the requirements for the degree of

Master of Science

University of Pittsburgh

2016

UNIVERSITY OF PITTSBURGH

SWANSON SCHOOL OF ENGINEERING

This thesis was presented

by

Wenfu Wang

It was defended on

March 31, 2016

and approved by

Ian Nettleship, PhD, Associate Professor

Department of Mechanical Engineering and Materials Science

Jung-kun Lee, PhD, Associate Professor

Department of Mechanical Engineering and Materials Science

Markus Chmielus, PhD, Assistant professor

Department of Mechanical Engineering and Materials Science

Thesis Advisor: Ian Nettleship, PhD, Associate Professor, Department of Mechanical Engineering and Materials Science

THE EFFECT OF CALCIUM ADDITION ON THE DISSOLUTION OF HYDROXYAPATITE

Wenfu Wang, M.S.

University of Pittsburgh, 2016

Hydroxyapatite (HA) has been widely used as a scaffold material for bone tissue engineering. It has an excellent biocompatibility but a low biodegradability. The calcium content in HA is thought to have an important effect on the degradation of the scaffold. The purpose of this thesis was to fabricate a highly porous HA foam using an emulsion direct foaming method by infiltration of calcium salt solution with different calcium concentration (2mol/L and 5mol/L) and sintering process. After that foam were immersed in Tris-bufffer Saline (TBS) at several different time points. We investigated the influence of infiltrated calcium salt in terms of their effects on weight loss/gain, surface morphology, and microstructural-level degradation with SEM observation and micro-CT. Interestingly there were a large amount of precipitation of calcium phases and detectable weight gain for the 2M samples. And for 5M samples, weight loss with time and a better dissolution behavior were observed.

TABLE OF CONTENTS

LIST OF TABLES

LIST OF FIGURES

ACKNOWLEDGEMENTS

My deepest gratitude goes first and foremost to Prof. Nettleship, my advisor, for his constant guidance and encouragement, helped me to coordinate my master thesis.

Second, I would like to express my heartfelt gratitude to Qinghao Zhang, who taught me many laboratory skills and instructed me a lot in the past two years.

Last my sincere appreciation would go to Prof. Chmielus and his group, for the help in micro-CT.

1.0 INTRODUCTION

Tissue engineering is one of the main approaches to tissue replacement such as bone repair[1] and heart transplantation [2] . The bone marrow transplantation includes bone marrow cell transplantation and hematopoietic stem cells transplantation (HSCT). HSCT was first developed in the 1950s and has become the most effective therapy for leukemia[3]. Besides that HSCT is also used in treatments for blood cancers and multiple myeloma. According to the survey conducted by the Worldwide Network for Blood and Marrow Transplantation, 51,536 hematopoietic stem cell transplantations were reported to have occurred in 72 countries in 2008[4]. However there are several problems in clinical application for HSCT. Allogeneic (the stem cells come from the donor) HSCT has the incidence of graft-versus-host disease because the cells in the host body may be attacked by the white blood cells from the donor[5]. Although autologous (the stem cells come from the patient) HSCT can avoid this problem, this option is inhibited by the low availability of the patients own HSCs for re-implantation that mean it is difficult to obtain an enough number of HSCs from the patient after a partial or complete bone marrow ablation[6].

Scaffolds are widely used biomaterials in bone tissue engineering, they can be synthesized in the laboratory using varieties of chemical approaches. Biocompatibility and biodegradability are the two most important requirements. Biocompatibility promotes cell adhesion and proliferation while biodegradability allows the replacement of scaffold with natural tissues and degradation into nontoxic products that can be resorbed by human body. In order to

simulate trabecular bone in clinic application, biomaterials scaffolds should be able to offer a similar structure and chemical microenvironment to trabecular bone. Macroporous calcium phosphate foams with high porosity and large open pore architectures should be the appropriate biomaterial for bone marrow cell culturing and bone reconstruction. Hydroxyapatite has a similar chemical composition to the inorganic phase of human bone. It has been widely used as artificial bone and bone substrate because it has a great bioactivity and biocompatibility. But the low biodegradability of HA impedes bone ingrowth and limits the application of HA as a scaffold biomaterial.

This thesis is based on the hypothesis that by introducing Ca rich phases, Ca infiltration of porous HA foams has the ability of increasing the solubility of the foams during bone marrow culturing. In particular, the ability of the calcium rich phases to induce the fragmentation of HA foams was studied.

2.0 BACKGROUND

2.1 REGENERATIVE MEDICINE

Regenerative medicine is defined as the fast developing interdisciplinary field of clinical therapies for the reconstruction, repair, replacement or regeneration of missing or damaged cells, tissues or organs, to restore its native architecture or function[7]. It includes cell therapy, gene therapy, tissue engineering and other methods that have enormous potential to treat and cure diseases[8].

2.1.1 Cell Therapy

Cell therapy can be defined as therapy in which cellular material is injected into a patient[9]. There are two branches of cell therapy, one is transplanting human cells from a donor to a patient which is established and legitimate, and the other is injecting animal cells into humans to treat disease which is much more dangerous. The origins of cell therapy can perhaps be traced to the nineteenth century, when Charles-Édouard Brown-Séquard (1817–1894) injected animal testicle extracts in an attempt to stop the effects of aging[10]. Although such attempts produced no positive benefit, further research in the mid twentieth century found that human cells could be used to help prevent the human body rejecting transplanted organs, leading in time to successful bone marrow transplantation[11].

2.1.2 Tissue Engineering

Tissue engineering is the use of a combination of cells, engineering and materials methods, and physicochemical factors to improve or replace biological functions. Although most definitions of tissue engineering cover a broad range of applications, in practice the term is closely associated with procedures that repair or replace portions of or whole tissues (i.e., muscle, skin, blood vessels, bladder, bone, cartilage etc.).

2.1.3 Biomaterials

A biomaterial is any surface, matter, or construct which interacts with living systems. Scaffolds are widely used biomaterials in bone tissue engineering, they can be synthesized in the laboratory using varieties of chemical approaches. Scaffolds must fulfill a range of requirements such as appropriate mechanical strength and stiffness, bioactive behavior, interconnected pore structure and bio-resorb-ability at predetermined rates[12]. Biocompatibility and biodegradability are the two most important requirements of scaffold materials, biocompatibility promotes cell adhesion and proliferation, while biodegradability allows the replacement of scaffold with natural tissues and degradation into nontoxic products that can be excreted or resorbed by human body. Porosity is another requirement of scaffolds, to accommodate cell reproduction and differentiation in tissues formation. Porosity plays an important role in regulating the bioactivity of a scaffold because of its influence on structural permeability that controls the initial rate of bone regeneration and also impacts the local mechanical environment experienced by the cells which mediates the equilibrium volume of new bone within the repair site[13]. Moreover, the scaffold should be capable of being formed into the desired shapes for use in a particular repair

site and sterilized for clinical use. Generally the biomaterials used to construct these porous scaffolds include: (i) synthetic biodegradable polymers such as poly (glycolic acid) (PGA), poly (lactic acid) (PLA), and their copolymer poly (DL-lactic-co-glycolic acid) (PLGA), and naturally derived polymers such as collagen and (ii) synthetic ceramics such as calcium phosphates[14]. Among the calcium phosphate, Hydroxyapatite (HA) and β-tricalcium phosphate (β-TCP) are the major phases used for culturing human mesenchymal stem cells (MSC) necessary for bone formation. Their similarity in composition and structure to the mineral phase of bone provides both high bioactivity and biocompatibility. Comparing with tricalcium phosphate, Hydroxyapatite is more effective at osteoconduction but has lower biodegradability. In consequence, biphasic mixtures of Ha and TCP are commonly used to achieve the best combination of osteoconduction and biodegradation.

2.1.4 Bioreactor

In the context of cell expansion or tissue formation, bioreactors may be defined as a device or system meant for growing cells or tissues. In tissue engineering and biochemical engineering, there are mainly two types of bioreactor stirred tank and the perfusion. A typical stirred-tank bioreactor is shown in Figure 2.1. Stirred tank bioreactor can be used to expand cell numbers and produce cell aggregates in dilute conditions. If a scaffold is used the cells are seeded by convection in the liquid medium. In the tank, the growth medium is continuously refreshed and filters are used to ensure the cells remain in the bioreactor core. The great advantage of stirred tank bioreactor over static culture is efficient perfusion of the cells and effective mixing of the media. This avoids the sharp changes in media concentration when media is periodically replaced during static culture. However the central portions of unvascularized scaffolds will be

subject to a different local media environment compared to the external surfaces of the scaffold when one relies on convection to transport media into the interior of scaffolds in a stirred tank bioreactor[15]. Consequently larger scaffolds can remain acellular in their interior. Furthermore, mechanical shear generated in the fluid of a stirred tank bioreactor can effect cell surface marker expression and result in undesirable effects on the culture[16]. In bone marrow researches, stirred tank bioreactors have been proved more successful in hematopoietic stem cell and progenitor expansion than static culturing[17]. To some degree, stirred tank reactors can allow the formation of multi-cell aggregates, especially with microcarriers which accommodate the requirements of adherent cell populations. For example, embryonic stem cells have shown greater expansion in stirred tank bioreactors compared to static culturing both as aggregates and in microcarriers[18].

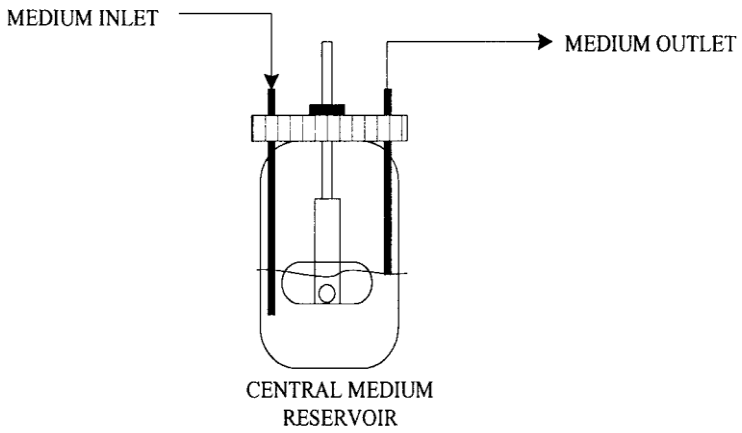

Figure 2.1. Stirred tank bioreactor

The other type of bioreactor is the perfusion bioreactor that include packed bed reactors and hollow fiber membrane reactors such as the one shown in Figure 2.2. Perfusion bioreactors are a better representation of physiological conditions in the body because cells are immobilized in a reactor core and media is perfused around them. In comparison with stirred tank bioreactors

uniform perfusion of the cells can be more difficult to accomplish in perfusion bioreactors and is quite sensitive to the architecture of the core. In principle, perfusion bioreactors offer the potential for controlled tissue formation from multiple cell types if the perfusion is controlled at sufficiently small length scales. Generally perfusion bioreactors can be classified as two dimensional bioreactors and three dimensional bioreactors. Three dimensional bioreactors are further differentiated into two types including direct perfusion systems and hollow fiber membrane reactors. In respect to stem cells research, three dimensional perfusion systems have achieved notable success in culturing of mesenchymal stem cells. For example, the mesenchymal stem cells have been shown to retain their multi-lineage potential in three dimensional perfusion bioreactors than static system[19].

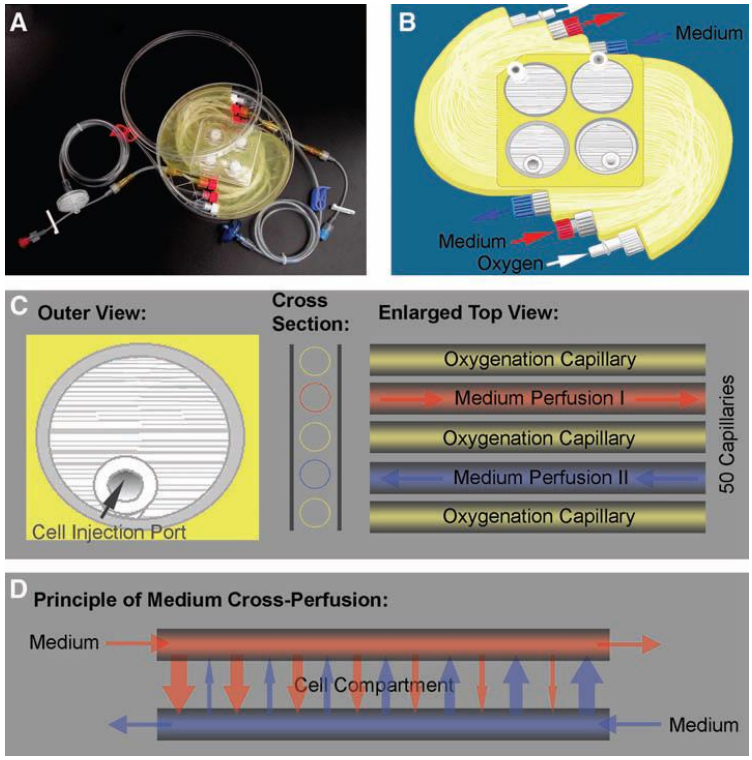

Figure 2.2 Perfusion geometry for hollow fiber membrane reactor

2.2 BONE MARROW

The mineral phase of bone consists of hydroxyapatite $Ca_{10}(PO_4)_6(OH)_2$ crystals deposited within a relatively small amount of organic matrix (~95% is type I collagen)[20]. There are two main types of bone architecture: cortical bone and trabecular bone (Figure 2.3). Cortical bone, also called compact bone, is commonly the hard outer layer on large bone that is responsible for structural integrity. The osteon is the main anatomical and functional unit of cortical bone. Each osteon is composed of concentric layers, or lamellae, of cortical bone that surround a central canal called the Haversian canal[21]. Cortical bone provides several of the structural functions of bone, such as supporting the whole body, protecting organs, providing levers for movement, and storing and releasing important physiological elements, particularly calcium. The other type is trabecular bone which is also called cancellous bone or spongy bone. Trabecular bone is highly porous and fills the interior of the large bones. Trabecular bone is highly vascularized and often includes red bone marrow where hematopoiesis, the production of blood cells, occurs. Trabecular bone is far less dense than cortical bone and contributes about 20% of the weight of a human skeleton.

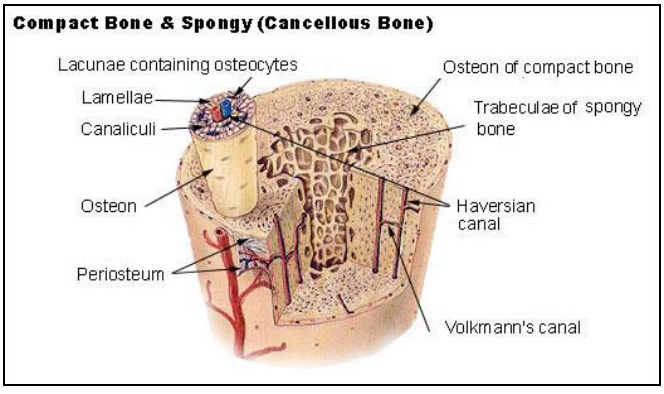

Figure 2.3 Cortical bone & trabecular bone

Bone marrow is the flexible tissue in the interior of trabecular bones and constitutes 4% of the total body mass of humans on average. There are two types of bone marrow, one is red marrow which is mainly made up of hematopoietic tissue and the other is yellow marrow which consists of fat cells (Figure 2.4). Red marrow contains red blood cells, platelets, and white blood cells and both types of bone marrow contain a plentiful number of blood vessels and capillaries. All the bone marrow of a new born baby is red marrow, but then some is converted to yellow marrow during growing and only about half of the bone marrow is red when he/she becomes an adult.

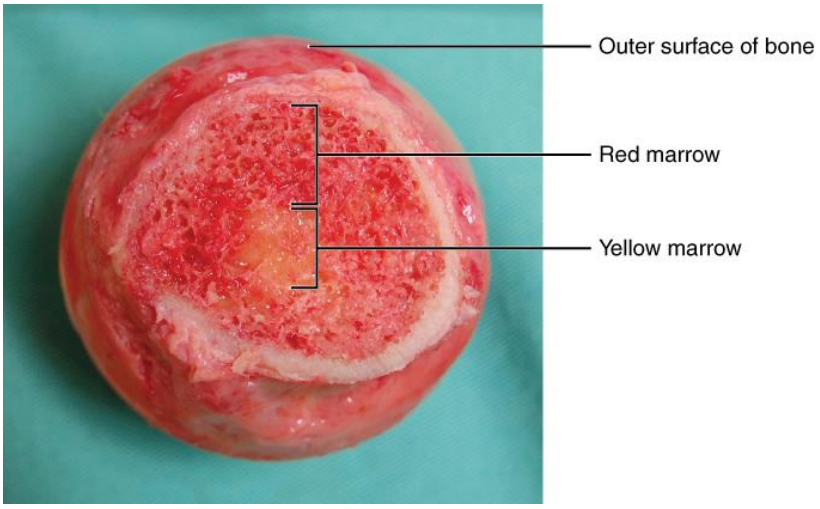

Figure 2.4 Red marrow and yellow marrow

2.2.1 Hematopoietic stem cell

Hematopoietic stem cells (HSCs) are the stem cells that generate all the other blood cells and immune system cells in the body through the process of hematopoiesis. They are derived from the mesoderm and located in the red bone marrow. Differentiation into progenitors and mature

cells and self-renew define the core function of HSCs. HSCs are able to replenish all mature blood cell types and also replenish their number with the same or very similar potential[22](Figure 2.5). Importantly, a small number of HSCs can expand to create an enormous number of daughter HSCs and progenitors [23] . This phenomenon is widely used in bone marrow transplantation in which a small number of HSC can be used to reform entire the hematopoietic system. This process shows that symmetrical cell divisions into two daughter HSCs must happen to a large extent. In order to keep steady state levels in the peripheral circulation, the HSCs produce 10^{11}–10^{12} blood cells every day and use the bone marrow vasculature as a conduit to the body's circulation system[24]. Stem cell self-renewal also occurs in the stem cell niche within the bone marrow. Related studies have showed that there appear to be two kinds of HSCs. If bone marrow cells from the transplanted from one person to another person and restore their hematopoietic system of an extended period, they are recognized as long-term HSCs that are capable of self-renewal[25]. Other HSCs which can regenerate all the types of blood cells but cannot self-renew over the long term under normal circumstances, are considered as short-term HSCs, progenitor or precursor cells.

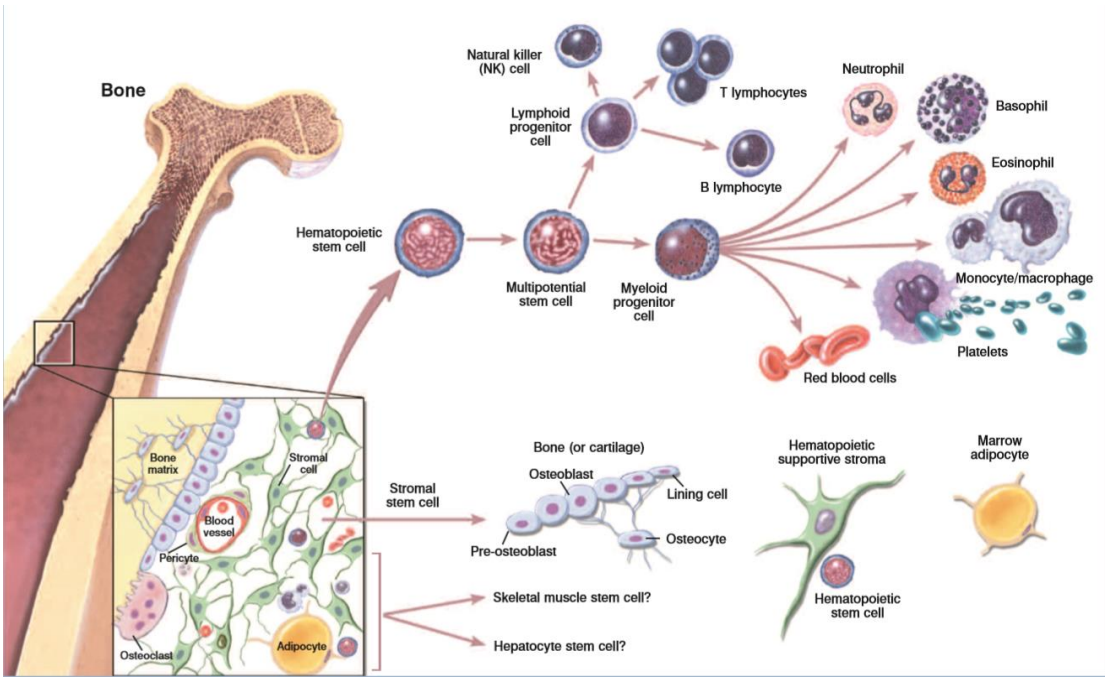

Figure 2.5 Hematopoietic differentiation

2.2.2 Hematopoietic stem cell transplantation

Bone marrow is the best known location for HSCs, and bone marrow transplantation has become synonymous with hematopoietic cell transplantation. Hematopoietic stem cell transplantation (HSCT) is the transplantation of multipotent hematopoietic stem cells, derived from not only bone marrow but also peripheral blood in the circulation system and umbilical cord blood sources. This transplantation is often performed for patients with some cancers of the blood or bone marrow, such as multiple myeloma or leukemia[26].

HSCT can be divided into two kinds, autologous (the stem cells come from the patient) and allogeneic (the stem cells come from the donor). Autologous HSCT requires that the stem cells should be stored in a freezer after being extracted from the patient. Then the patient is treated with high dose chemotherapy with radiotherapy resulting in partial or complete bone

marrow ablation, which means patient's bone marrow's ability to grow new blood cells will disappear. After that the stored stem cells are thawed and transfused into the patient, the destroyed tissue will be replaced with new bone marrow and the normal blood cell production will be resumed. Autologous transplants have lower risk of infection during the immune-compromised section of the treatment because the immune function is able to recover quickly. Additionally, the incidence of graft-versus-host disease (GVHD) is very rare since the recipient and donor is the same individual. These advantages have established autologous HSCT as one of the standard second-line treatments for such diseases as lymphoma[27]. However, for other cancers such as acute myeloid leukemia, the autogenous HSCT may have a higher possibility of cancer relapse and related mortality compared with allogeneic HSCT, therefore the allogeneic treatment may be better for those conditions[28].

In allogeneic HSCT, stem cells are extracted from the (healthy) donor and then transplanted into the (patient) recipient. Allogeneic HSC donors must have a tissue type that matches the recipient based on the variability at three or more loci of the human leukocyte antigen (HLA) gene[29]. The recipient will still need immunosuppressive medications to minimize graft-versus-host disease (GVHD) even though there is a good match at the critical alleles[30]. Allogeneic transplant donors may be related, syngeneic or unrelated to recipients. In generally, by transplanting healthy stem cells to the recipient's bloodstream to reform a healthy immune system, allogeneic HSCTs can improve chances for cure or long-term remission once the immediate transplant-related complications are resolved[31 32 33]. Doing additional HLA-testing from the blood of potential donors is the way to find a suitable donor. The HLA genes split into two categories (Type I and Type II). Generally, mismatches of the Type-I genes increase the risk of graft rejection while mismatches of the Type II gene increases the risk of graft-versus-host

disease (GVHD). In addition, even a mismatch as small as a single DNA base pair is significant, therefore the knowledge of the exact DNA sequence of the genes for both donor and recipient is required. Indeed, if bioreactors could be used to expand the supply of available bone marrow stem cells and progenitors to clinically relevant amounts, greater flexibility would be achieved for transplantation services.

2.3 CALCIUM PHOSPHATE

2.3.1 Hydroxyapatite

Hydroxyapatite (HA) is a naturally occurring mineral form of calcium apatite, its formula is $Ca_5(PO_4)_3(OH)$ but it is generally written as $Ca_{10}(PO_4)_6(OH)_2$ to show that the crystal unit cell comprises two formula units. Hydroxyapatite has a hexagonal crystal structure with space group P63/m and 44 atoms per unit cell. Stoichiometric HA has a Ca/P ratio of 1.67, and unit cell dimensions of a=b=9.432Å and c=6.881Å. The structure of an HA unit cell is shown in Fig. 3.1.

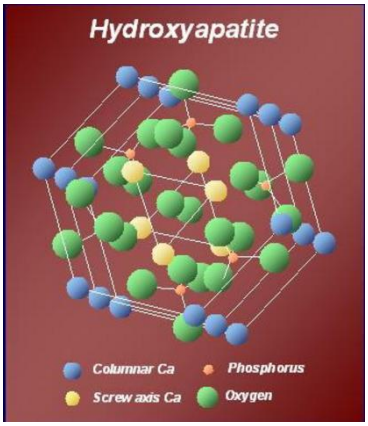

Figure 2.6 Crystal structure of HA[34]

Hydroxyapatite is the hydroxyl endmember of the complex apatite group. The OH^- ion can be replaced by chloride, fluoride, or carbonate, forming chlorapatite or fluorapatite[35]. Pure hydroxyapatite powder is white. Naturally existing apatites can also have grey, yellow, brown, or green colorations, comparable to the discolorations of dental fluorosis.

Hydroxyapatite (HA) has a similar chemical composition to the inorganic phase of human bone and teeth[36]. HA is widely used in biomedical area for its bioactivity and biocompatibility. But HA has some poor mechanical properties such as the brittleness and low fracture toughness, which can limit its applications to non-load bearing or metallic implant surfaces coating[37]. The tensile strength of the synthetic dense HA and cortical bone are respectively 68.49-191.78 Mpa and 68.49 Mpa, and the compressive strength of the synthetic dense HA and cortical bone are 205.48-890.41 Mpa and 136.99 Mpa[38]. In addition the Young's Modulus of cortical bone is $1.38x10^4$ Mpa, while that of HA is $3.42\text{-}10.27x10^4$ Mpa. HA is also harder than bone and bulk HA implants have low reliability under tensile loading possibly can result in catastrophic failure in clinic use. Some improvement in the mechanical properties of HA ceramics, has been achieved by making composites and controlled microstructures via different sintering techniques and nanostructured powders[39]. However, the improvements have been limited.

As a bioactive material, the most important advantage of HA is that a direct chemical bond can be achieved between bone and HA implants without the formation of a collagen interface layer which usually occurs on many other bio-inert materials after implantation[40]. The bond strength between HA and bone is much higher than between bone and other materials because of the direct chemical bonding. In addition there is no fibrous tissue capsule between the implant and bone which is significant for the patient's recovery after implantation[41].

HA degradation rate is not strongly related to processing variables including: purity, HA form (bulk form, porous form, coating, and HA/polymer composites), microstructure, implant site and body conditions[42]. Indeed, the rate of resorption of HA is generally considered to be too low to allow timely restructuring of the tissue in the scaffold and so materials with faster degradation rates, such as TCP, have been incorporated into biphasic calcium phosphate scaffolds.

2.3.2 Tricalcium phosphate

Tricalcium phosphate (TCP) is a calcium salt of phosphoric acid, its chemical formula is $Ca_3(PO4)_2$. It is also called tribasic calcium phosphate and bone phosphate of lime (BPL). Tricalcium phosphate has three crystalline polymorphs, β-TCP, α- TCP and α′-TCP, depending on temperature[43]. The α′-TCP is stable only in equilibrium at temperatures higher than 1430 ^{O}C and converts back to α-TCP below the transition temperature. The β-TCP and the α- TCP forms can both be achieved at room temperature even though the transition from β-TCP to α- TCP occurs at 1125 ^{O}C[44]. The β-TCP has a crystallographic density of 3.066 g cm^{-3}, the α-TCP has a density of 2.866 g cm^{-3} and α'-TCP has a density of 2.702 g cm^{-3}.

β-TCP has a rhombohedral structure with unit-cell parameters a=b=10.4352Å, c=37.4029Å, α=β=90°, and γ=120° in the hexagonal setting (space group R3c)[45]. There are 273 atoms or 21 formula units per unit cell. α-TCP has a monoclinic structure (space group $P2_1/a$) with unit-cell parameters a=12.8328 Å, b=27.1958 Å, c=15.1656 Å, α=γ=90° and β=126.2°. Each unit cell contains 312 atoms or 24 formula units. All kinds of TCP are described as containing "columns" of cations and anions. The α-TCP consists of two types of ion columns aligned along the (0 1 0) direction, as shown in Figure 2.7a. Column A consists of Ca^{2+} ions and

column B consists of Ca^{2+} and PO_4^{-3} ions. The crystal structure of β-TCP can be described by A and B columns, running along the c-axis[46] (Figure 2.7). Each A column is surrounded by six B columns, while each B column is surrounded by two A and four B columns.

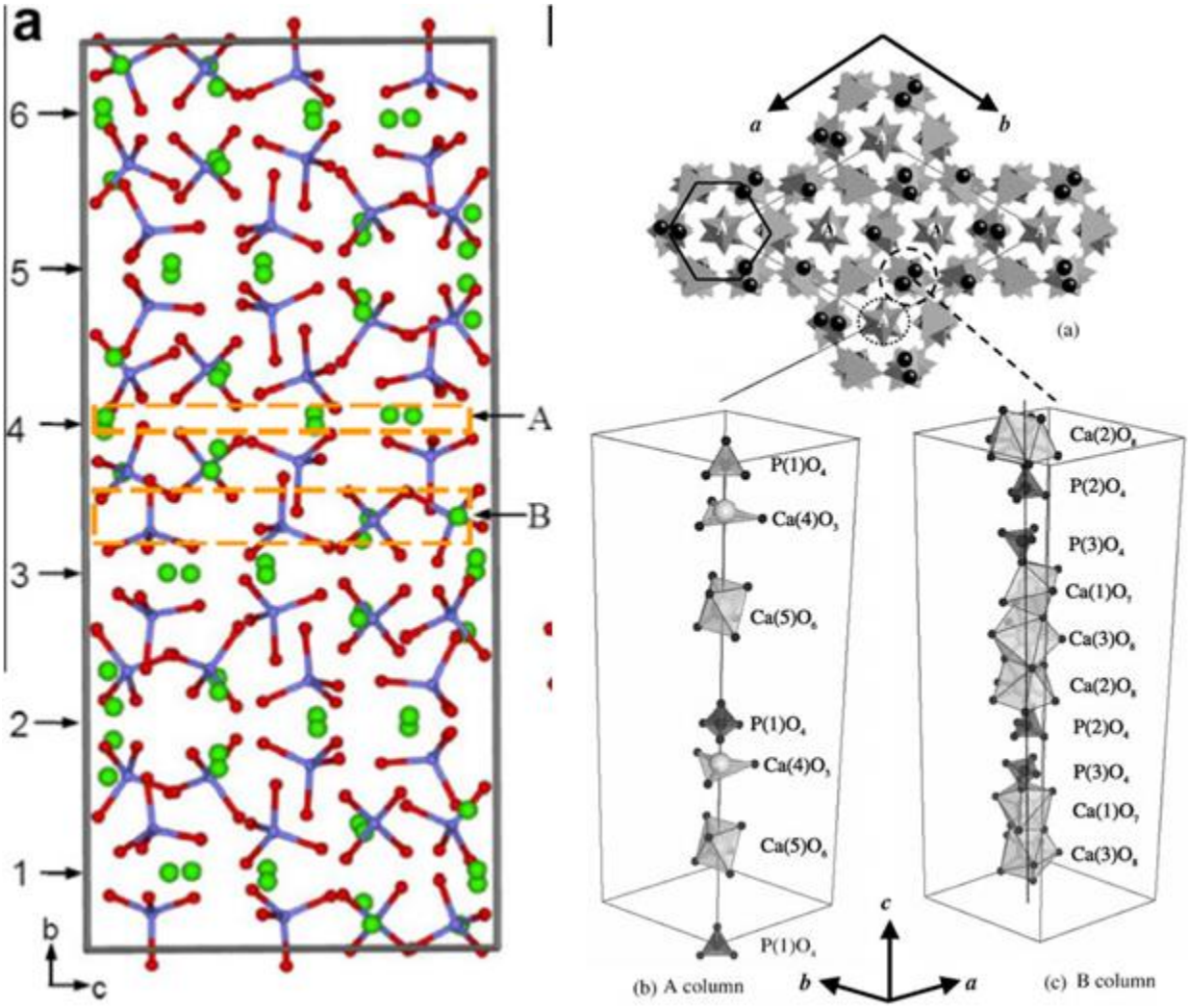

Figure 2.7 Crystal structure of α-and β-TCP[45]

Some related studies have shown that β-TCP is mechanically stronger than α-TCP, for the reason that some bonds of PO_4 groups formed in β-TCP are stronger than the bonds of α-TCP. In clinic application(dentistry, orthopedic surgery, bone repair, etc.), β-TCP is more widely

used as biomaterials such as macro-porous bioceramics, while α-TCP is usually used as a fine powder for calcium phosphate cements due to its higher solubility and biodegradability[47,48].

2.3.3 Solubility of HA and TCP

Calcium phosphates can be remodeled by the osteoblasts and osteocytes in biological processes. These materials can also dissolve in aqueous solution. In the dissolution process, Ca^{2+} ions and PO_4^{3-} ions are released from the ceramic scaffold into the solutions and eventually influence the cell culture environment. Calcium is known to influence cells residing in the bone marrow niche cells, such as osteoblasts and endothelial cells[49]. Therefore a calcium phosphate scaffold can affect the HSC niche and HSC fate by releasing calcium. This is the reason that solubility of calcium phosphates can be important to culturing HSCs on scaffolds in clinic application.

Many factors affect the dissolution behavior of HA, β-TCP, α-TCP, such as the technique of preparation, phase content, density and the extent of ionic substitutions into the apatite lattice and microstructure[50,51]. Fig. 3.3 shows solubility of calcium phosphates with different Ca/P ratio as a function of pH. From the figure, it is obvious that the order of solubility is α-TCP>β-TCP> HA. At pH=7.3, which is general bone marrow culture pH condition, calcium carbonate has a solubility at around $10^{-2.5}$ which is highest solubility in the calcium phosphates. Then it was followed by Tetracalcium phosphate (TeCP) and α-TCP. The solubilities of these two phases are about the same that is $10^{-2.6}$. The solubilities of β-TCP and HA respectively are$10^{-3.5}$ and $10^{-4.3}$.

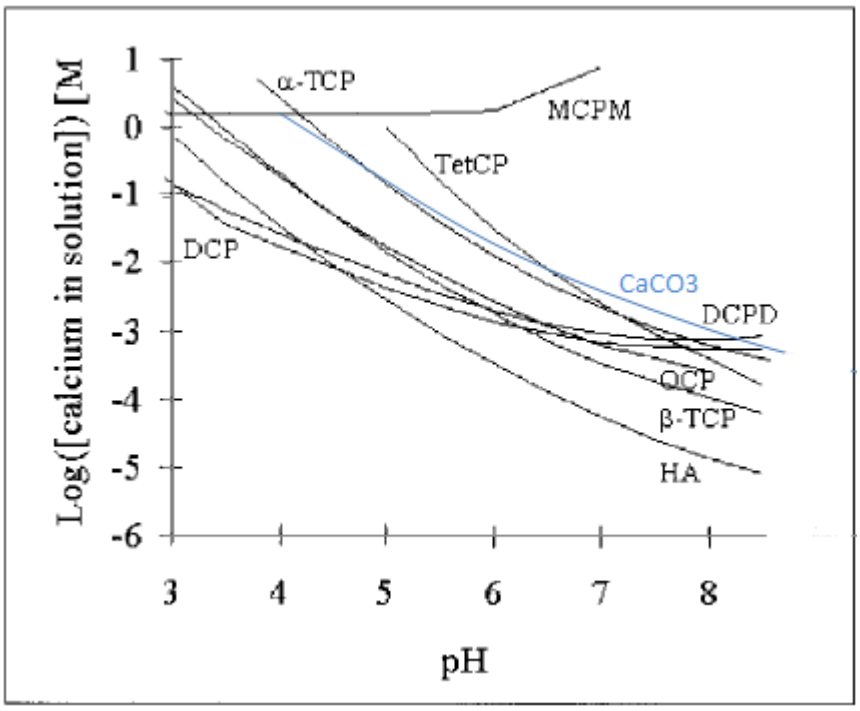

Figure 2.8 Solubility isothermal of calcium phosphates with different Ca/P ratio in water[52]

2.4 PROCESSING OF MACROPOROUS CERAMIC FOAMS

Trabecular bone consist of macroporous (55-70% interconnected porosity) calcium hydroxyapatite (HA)[53]. The macroporosity in the trabecular bones promotes the ingrowth of the soft tissues and vascularization of the bone marrow. In order to simulate trabecular bone in clinic application, biomaterials scaffolds should be able to offer a temporary support for the cells facilitate cell attachment. Additionally, the scaffold also needs to provide a similar chemical microenvironment to trabecular bone. Macroporous calcium phosphate foams with high pore fractions (greater than 80%) and large open pore architectures should be the appropriate biomaterial for bone marrow cell culturing as well as bone repair and reconstruction.

Porous materials are classified into three types depending on the pore diameter d: macro-porous (d>50 nm), meso-porous (50 nm>d>2 nm) and microporous (d>2 nm), on the basis of the nomenclature of IUPAC (International Union of Pure and Applied Chemistry)[54]. Most attention is placed on the fabrication of open macroporous bioceramics because the pore network allows the tissue to infiltrate, which further promotes the attachment between the implants and tissues in bone repair[55]. In a porous form, hydroxyapatite ceramics can be colonized by bone tissue with the same characteristics as peri-implanted tissues[56]. According to some researchers, the pore size must be larger than 50-100 μ m or even 250-300 μ m to insure vascularization[57].

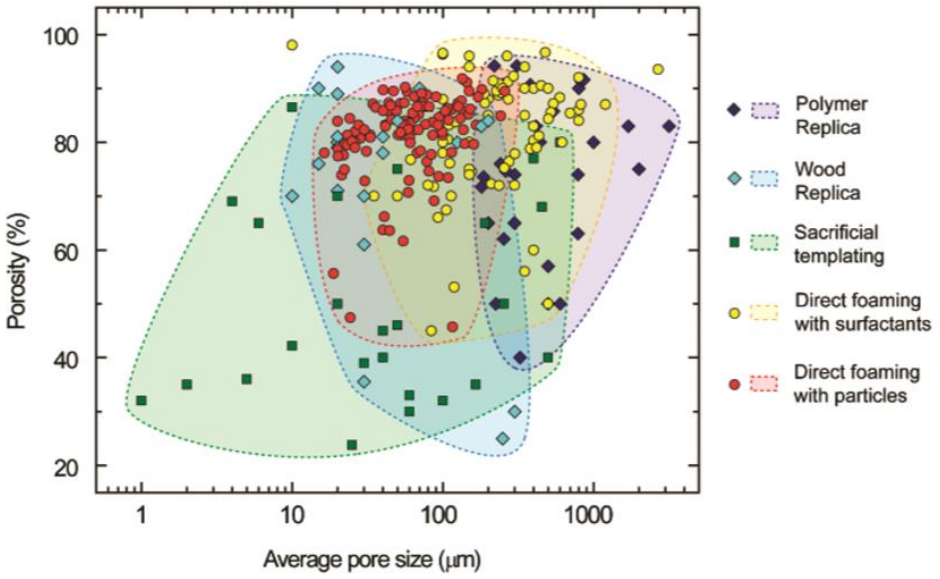

Figure 2.9 Typical porosity and average pore size achieved via the replica, sacrificial templating, and direct foaming processing methods[58]

The most straightforward and conventional processing approach for the preparation of porous bioceramics is the partial sintering[59]. But this method often results in a relatively low

porosity (<60 vol%), with pores homogeneously distributed within the microstructure. This low porosity is not suitable for bone tissue ingrowth. Thus many novel methods for the preparation of macroporous ceramics with controlled microstructure have been developed recently. Figure 2.9 shows typical porosity and average pore size achieved via different processing routes. The processing methods described in this chapter are classified into replication, sacrificial templating and direct foaming methods, as schematically illustrated in Figure 2.10.

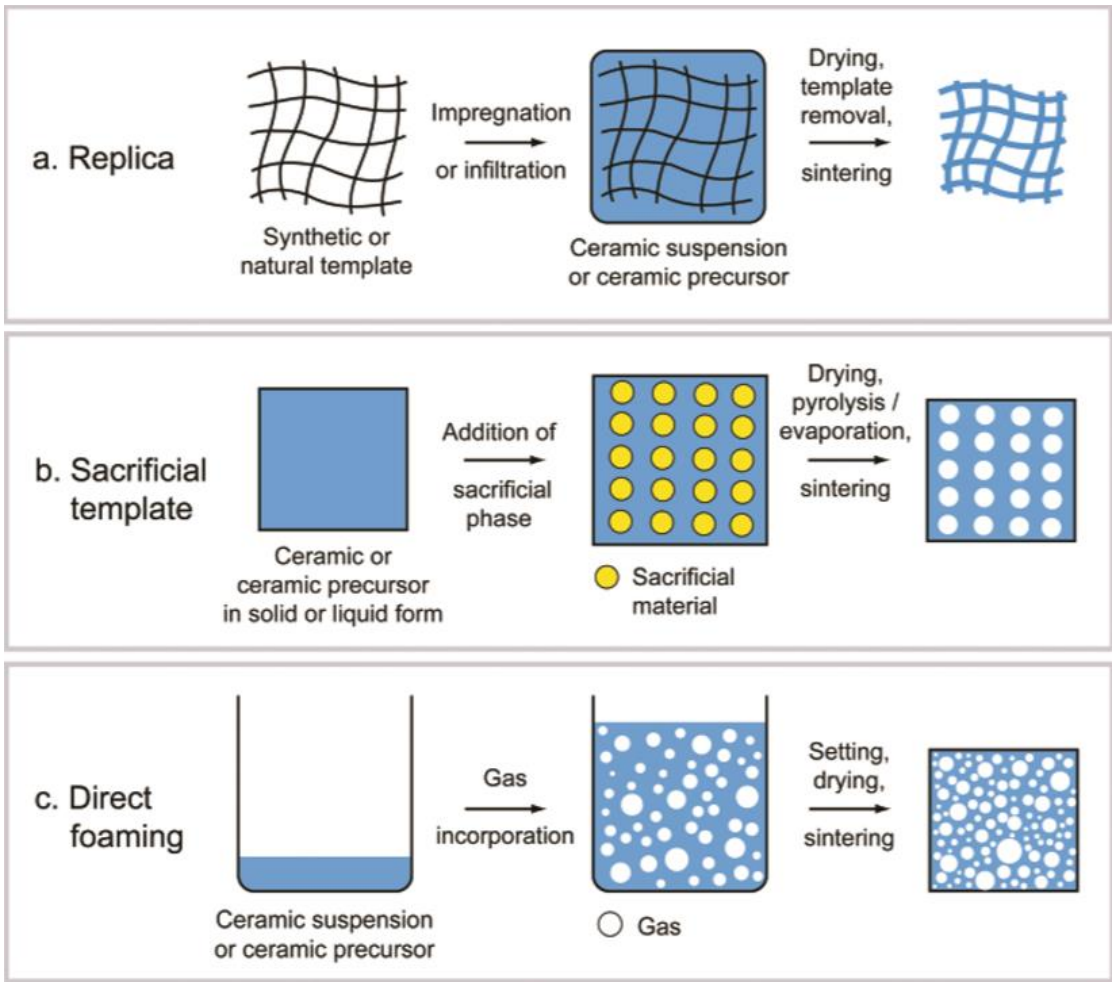

Figure 2.10 Scheme of three main processing routes for macroporous ceramics[60]

2.4.1 Replication

The replication method is based on the impregnation of a preexisting cellular architecture, usually a polymer foam, with a ceramic suspension or precursor solution in order to fabricate a macroporous ceramic with the same morphology as the original porous material (Fig. 4.2(a)). Synthetic and natural cellular structures are two types of templates to fabricate macroporous ceramics. In the polymer replica approach, a highly porous polymeric sponge is soaked into a ceramic suspension till the ceramic material fills in the internal pores. Then roller compression is applied to the impregnated sponge to remove the redundant suspension and enable a thin ceramic coating to form over the struts of the original cellular structure. After that the polymeric template is dried and pyrolyzed through careful heating between 300℃ and 800℃. Finally the ceramic coating is sintered in an suitable atmosphere at temperatures ranging from 1100℃ to 1700℃ (depending on material) after the polymeric template was removed.

Porous ceramics obtained with the sponge replication method can achieve total open porosity levels within the range 40%–95% and the interconnected pores can reach the sizes from 200 μm to 3 mm[61]. In replication methods, a variety of ceramic cell types can be fabricated, including open-cells, semi-closed cells and closed-cells[49]. There is a disadvantage of the sponge replication method in that the struts of the reticulated structure are often cracked during pyrolysis of the polymeric template, signally degrading the final mechanical strength of the porous ceramic[62]. Some possible ways to avoid this have been discovered, such as using additives to improve the wetting of the suspension on the sponge[63], performing a second impregnation step to fill the cracks in the ceramic struts, and introducing fibers to improve the integrity of the material.

2.4.2 Sacrificial template method

The sacrificial template technique usually includes the preparation of a biphasic composite comprising a continuous matrix of ceramic particles (or precursors) and a dispersed sacrificial phase. The sacrificial phase is originally homogeneously distributed in the matrix and finally extracted to produce pores within the microstructure (Fig. 4.2(b)). In this approach, the sacrificial phase is intended to produce porous materials as a negative replica. The biphasic composite is usually prepared in three ways: (1) pressing the powder mixed as two components[64], (2) generating a two-phase suspension that is subsequently processed by wet colloidal routes such as slip, tape or direct casting[65], (3) impregnating previously consolidated preforms of the sacrificial material with a preceramic polymer or ceramic suspension[66]. The type of pore former employed decides the way of extracting the sacrificial material from the consolidated composite. Many kinds of sacrificial materials have been used as pore formers, such as natural and synthetic organics, salts, liquids, metals, and ceramic compounds. As pore formers, synthetic and natural organics are often extracted through pyrolysis by applying long thermal treatments at temperatures between 200℃ and 600℃[6768]. Liquids and oils can be evaporated or sublimated easily without the generation of unexpected toxic gases and residual stresses during the removal process[69 70]. Sacrificial materials such as salts, ceramic and metallic particles, are usually extracted by chemical rather than thermal approaches. Repeatedly washing the composite with water can simply achieve the extraction salts[71]. Ceramic and metallic particles or fibers need more aggressive agents and are usually extracted by acidic leaching[7273].

Compared with the other fabrication approaches, the main advantages of the sacrificial template method is that the porosity, pore size distribution, and pore morphology of the final

ceramic component can be decided by a suitable choice of the sacrificial material. With this method, ceramics with porosities and average pore sizes ranging from 20% to 90% and 1–700 μ m can be achieved.

2.4.3 Direct forming

In direct foaming methods, ceramics suspension which are foamed by incorporating air or gas, stabilized, dried, and subsequently sintered at high temperatures to obtain consolidated structures. In this method, highly porous ceramic materials (up to more than 95% porosity) can be easily produced with low cost. On one hand the porosity of ceramics is proportional to the amount of gas incorporated into the suspension during the foaming process. On the other hand the pore size is determined by the stability of the wet foam before setting takes place. Wet foams are thermodynamically unstable systems because of their high gas–liquid interfacial area. Foam destabilization is triggered by several physical processes to decrease the system free energy. The three main destabilization processes are drainage (creaming), coalescence (film rupture), and Ostwald ripening (disproportionation). The size of incorporated bubbles can be significantly increased by these destabilization processes, generating large pores in the final cellular microstructure. So the approach used to stabilize the air bubbles incorporated within the initial suspension is the most important issue in control of the direct foaming methods.

There are two predominant approaches stabilizing the bubble in ceramic suspension. One is to use surfactants which reduce the interfacial energy of the gas–liquid boundaries. But long-chain surfactants have difficulty preventing the destabilization of foams in a short time because the adsorption energy of surfactants at the gas–liquid interface is relatively low. Hence, a setting agent is also required to stablize the foam microstructure before extensive coalescence and

disproportionation can occur. The ultimate pore size of the foam depends on a balance between the kinetics of bubble disproportionation and the speed of liquid/suspension setting. There are different types of surfactants such as protein, anionic, cationic and nonionic. With the surfactant-based direct foaming method, pore sizes within the range of 35 μm to 1.2 mm can be achieved and porosity of cellular structures produced can be tuned from 40% to 97%. Compared with the replica method, the direct foaming methods usually produce dense flawless struts after sintering, increasing the mechanical strength of the porous ceramic.

The other approach of stabilizing the foam is using solid particles with tailored surface chemistry to stabilize gas bubbles. Particles adsorbed at the gas–liquid interface can prevent the destabilization mechanisms for several days, it is a long-term stabilization compared with the surfactants foaming method[74]. Due to its excellent stability, particle-stabilized foams can be directly dried and sintered to obtain the macroporous ceramic without a setting step. The porosity of foams produced with this method range from 40% to 93%, and the average pore sizes can be tuned from 10 to 300 μm. Closed-pore ceramics foams can be easily prepared with this method since the bubbles in the wet foam can be fully covered with a layer of surface modified particles.

2.5 SINTERING

Solid state sintering is the process of consolidating a mass of powder particles by the application of heat without melting[75]. The objective is to achieve the final ceramic part by elimination of all the pores contained in the body. During this process, densification of the shaped part is driven by reduction of the surface area of the powder and achieved by one of several mass transport processes. The densification mechanisms, including grain boundary diffusion and volume

diffusion, cause neck growth between touching particles and a reduction their center to center distance resulting in shrinkage and pore elimination. In contrast, coarsening mechanisms such as surface diffusion cause neck formation without a reduction in center to center distance and thereby reduce the surface area of the powder without shrinkage and pore elimination. It is therefore important to use very small powder particles that increase the driving force for solid state sintering and use a sintering temperature at which the densification mechanisms such as grain boundary diffusion or volume diffusion are dominant. Sintering is extraordinary important because the ultimate properties of the ceramic parts strongly depend on it. Fig. 5 shows the microstructural changes that occur during solid state sintering.

Pressureless sintering of HA is generally performed in the temperature ranging from 1100℃ to 1250℃. The sintering of HA powder compact, like all ceramics, can be divided in three sequential stages[76]. (1) In the initial stage, the interparticle necks form at contacts and grow. This stage occurs with a little or no densification, and it lasts till the relative density reaches 65% of the fully dense material. (2) In the intermediate stage, the necks have impinged and densification generally occurs by the shrinking of the pore channels at triple points. The pores remain open and form a continuous phase in intermediate stage sintering. This stage is the major part of sintering, and it ends when the pores pinch off to become isolated at grain corners. (3) In the final stage of sintering, the isolated pores may disappear, leaving a fully or nearly fully dense ceramic. During sintering of HA, densification occurs without formation of any liquid phase, and structural investigations reveal no evidence of secondary phases, crystalline or amorphous formed[77].

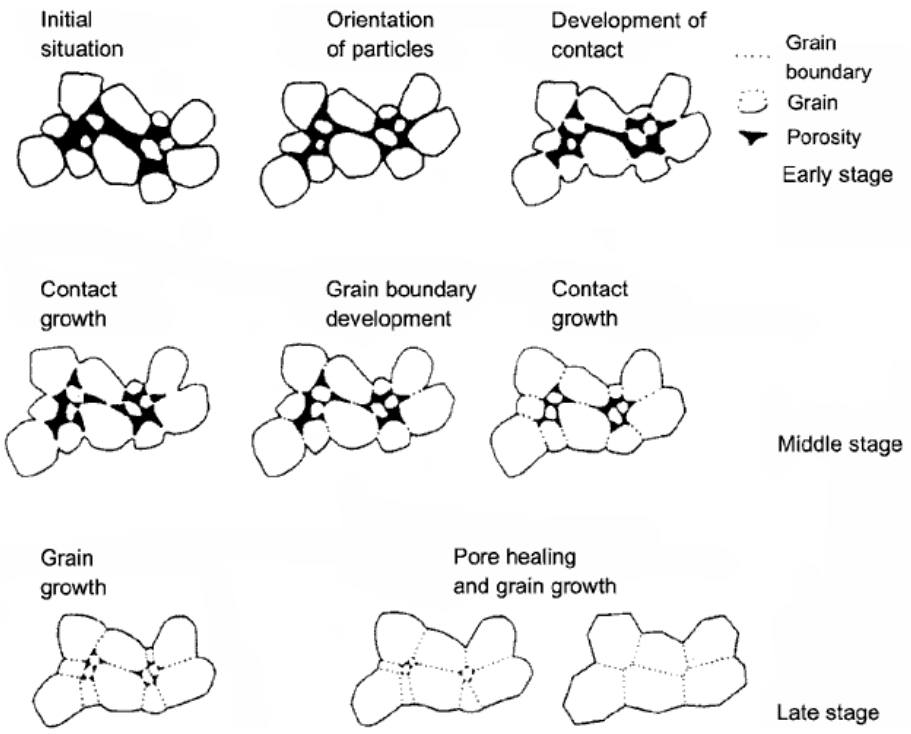

Figure 2.11 Grain growth during the sintering process[78]

2.6 INFILTRATION OF POROUS CERAMICS

Infiltration is the process of introducing a second phase into porous preforms with a liquid precursor that is converted into an inorganic phase during pyrolysis. The porous preforms should have an open-pore structure with high porosity to allow the liquid to pass into the interior. There are some advantages of using liquid infiltration processes. The preforms can be shaped with conventional methods. Then a variety of unique microstructures with particular mechanical properties, surface modification, and compositional gradients of the second phase can be achieved by controlling the infiltration processes[79]. In addition, the precursor can be used to

increase the relative density and strengthen a powder compact without shrinkage[80]. The advantages of the liquid infiltration technique have been used to fabricate various particulate-reinforced ceramic composites[81].

There are some infiltration studies showed in the following: Marple and Green fabricated alumina/mullite ceramic and indicated that the phase distribution and the microstructure development can be controlled by infiltration process[81]. After partial sintered at 1300°C, the alumina cylinder compacts were immersed in prehydrolysed ethyl silicate solution for several different periods of time, dried and heated at 1200°C to allow the decomposition of the ethyl silicate. Finally, the alumina cylinder compacts were heated at 1650°C to get densified and mullite was formed. Similarly, in Yung-Jen Lin's work, mullite was cyclically infiltrated into porous Zirconia[82]. In the process, the distribution of mullite was nonuniform, with higher mullite concentration near the external surface. After the infiltration and sintering, the gradient in second phase created residual stresses and cracking on cooling. This residual stress is thought to arise because of differential thermal expansion[83]. These studies support the idea that infiltration is an effective way to change the composition and microstructure of ceramic bodies[84].

Some research has showed the influence of Ca content on the degradability of HA[85]. Therefore Ca^{2+} infiltration of HA foams provides a feasible method to optimize the properties of calcium phosphate ceramics. In the preliminary work for this proposal, calcium nitrate solution was infiltrated into porous HA foam. Then the foam was immersed in ammonium hydroxide to form CaO particles in the HA foam before final sintering.

3.0 HYPOTHESIS

Calcium phosphate has become an important biomaterial for bone tissue growth. Different calcium phosphate phases with various ratio of Ca/P have different bioactivity and biocompatibility. Hydroxyapatite with Ca/P=1.67 is reported to enhance bone marrow cell culturing but the disadvantage is the low degradability compared with other phase of calcium phosphate. Recent studies have shown that a higher calcium content in hydroxyapatite scaffolds might improve the degradability of the scaffold.[81] And according to Hoppe Alexander's review, scaffolds with higher Ca concentration also enhance osteogenesis (growth of new bone) and angiogenesis (growth of new blood vessels)[86].

Therefore the hypothesis of this work is that by the infiltration with Ca into porous HA foams, the solubility of the HA foams during the bone cell culturing can be enhanced.

4.0 OBJECTIVES

1. Partially sintered HA foams will be infiltrated with calcium nitrate precursors to produce CaO or CaCO3 phase in the new ceramic foams.
2. The influence of Ca rich phase on structure during the dissolution will be investigated by SEM and micro-CT.

5.0 APPROACH

5.1 4.1 MATERIAL PREPARATION

5.1.1 Hydroxyapatite powder preparation

First hydroxyapatite powder (SIGMA-ALDRIVH Co) was calcined at 900°C for 1 hour to insure the purity. Then the powder was milled in water for 24 hours. Then the powder was dried and granulated by pestle and mortar.

5.1.2 High calcium phosphate ratio foam

A HA ceramic foam was fabricated by emulsion method and then infiltrated with Ca^{2+} solution in the following process to get a high calcium content.

First, ammonium polymethacrylate polyelectrolyte dispersant (Darvan C, RT Vanderbilt Co.) was added to deionized water and HCl was added to the solution adjusting the pH to 5.5. Second, the prepared HA powder was added to the suspension and it was stirred at 2500 RPM for 20 minutes to get appropriate dispersion and then the cationic surfactant (benzethonium chloride, Sigma) was added to the emulsion and stirred at 2500 RPM for 2 minutes. Last, 10% volume of heptane was added to the emulsion and stirred at high speed for 40 seconds. The recipe for making the foams is listed in Table 5.1 **The recipe for making HA foam**.

Table 5.1 The recipe for making HA foam

Volume% of HA	30%
Mass of HA	10g
Darvan C	2.9ml
Deionized water	4.48ml
heptane	1.172ml
Benzothonium Chloride	0.1776g

A paper mold was used to contain the emulsion and it was put in a fume hood for 2 hours with 60% humidity and the further dried for 24 hours with 40% humidity in order to allow the foam expand and generate connected pores. Then the mold containing the foam was heat treated in a furnace for 7.18 hours in 900°C using 2°C/minute heating rate and 10°C/minutes cooling rate. After that the foams were partially sintered in air at 1100°C for 1 hour to get an appropriate amount of strength and open porosity for infiltration.

The infiltrant was made with calcium nitrate tetrahydrate ($Ca(NO_3)_2 \cdot 4H_2O$, Alfa Aesar, England) and water. The solution concentrations were prepared with Ca^{2+} concentrations of 2mol/L and 5mol/L. The foams were then evacuated to remove the air from the open pores and then immersed in the infiltrant. After 24 hours the foams were removed from the calcium nitrate solution and immersed in ammonia hydroxide solution at pH=12.5 for 30 minutes to allow the Ca^{2+} to precipitate $Ca(OH)_2$ in the open pores of the foam. After that the foams were dried in air for 24 hours at room temperature and then was fired at 900°C to achieve insitu crystallization of CaO in the pores, and then sintered at 1300° C for 2.25 hour so the struts of the foam were fully

dense. The heat rate for sintering was 5°C/minute while cooling rate was 10°C/minutes. The open pore volume fraction in the foam was approximately 0.9.

Finally the foams were cut into small pieces, the weight of each sample is controlled in the range between 0.0390g and 0.0410g.

5.2 CHARACTERIZATION

In order to compare foams at before and after the solubility tests, micro-CT and SEM were the main methods used.

5.2.1 Micro-CT

In order to create cross-sections of a sample that can be used to recreate 3D renderings without destroying the original object, X-ray microtomography was used to scan all the samples before and after solubility test in the scanner called SKYSCAN 1272(Micro Photonics Inc.). Low resolution (1224x820) and copper filter were applied during the process. After scanning, a 3D image reconstruction program was used to achieve 2D individual slices through the samples. Then a program called CTAn (Micro-CT analysis) was used to measure particular parameters of each samples, such as volume, close pore number, porosity and pore size distribution.

5.2.2 SEM test

Scanning electron microscopy analysis was performed on the surface of the infiltrated sample foams including those subjected to solubility test (which will be discussed below) and untreated ones. The foams were coated with palladium using a sputter coater and examined in a Phillips XL30 scanning electron microscope, the magnification rage is from 50 to 20000.

5.3 STATIC SOLUBILITY TEST

Three groups of infiltrated foams with 0mol/L, 2mol/L, 5mol/L Ca^{2+} infiltration were prepared as described in Table 5.1. The samples were soaked in saline at room temperature. There were 7 time points (30minutes, 1 hour, 1 day, 3 days, 1 week, 2 weeks and 4 weeks) and 3 samples for each different infiltration concentration and each time point. The number of total samples was 63. All the samples were placed in separate sealed tubes which contained 2ml Tris-buffer Saline. Afterward the samples were removed from the saline after the appropriate immersion time. Then the foams were allowed to dry and they were coated with palladium and observed in SEM.

Table 5.2 Time points for each group under infiltration process with different Ca^{2+} concentration

	0.5hr	1 hr	1day	3days	1 week	2 weeks	4weeks
0mol/L							
2mol/L							
5mol/L							

6.0 RESULTS AND DISCUSSION

6.1 WEIGHT CHANGE

The weight of each foam was measured before and after the solubility test. And the weight change percentage was calculated. According to the data, a line chart with error bar was drew (Figure 6.1). As shown in the plot, the line representing the samples infiltrated with 5mol/L Ca^{+} solution indicates the weight of the samples tends to decrease with time while the HA line shows that the weight change of pure HA foams tends to increase with the time from 30 minutes to 1 week then decrease with time. And the line representing 2M samples indicates that the weight change has the similar trend as pure HA but not notable. It is apparent that the trends are comparable to the size of the error bars. This is probably because the samples are small and the overall change in weight is less than 2% suggesting very small changes in weight and the interpretation is affected by the variation between the repeats and the same time point. Afterwards, analysis of variance (ANOVA) was used to analyze the data of weight change. According to the ANOVA result, at the time point of 3 days, 2 weeks and 4 weeks, the weight change percentage of HA samples is significantly higher than that of 5M samples meanwhile the weight change percentage of 2M samples is significantly higher than that of 5M samples at the time point of 2 weeks. It is clear that 5mol/L infiltration creates different behavior with a weight

loss whereas the HA and 2mol/L infiltrated samples tend to show a weight gain within the first 400 hours.

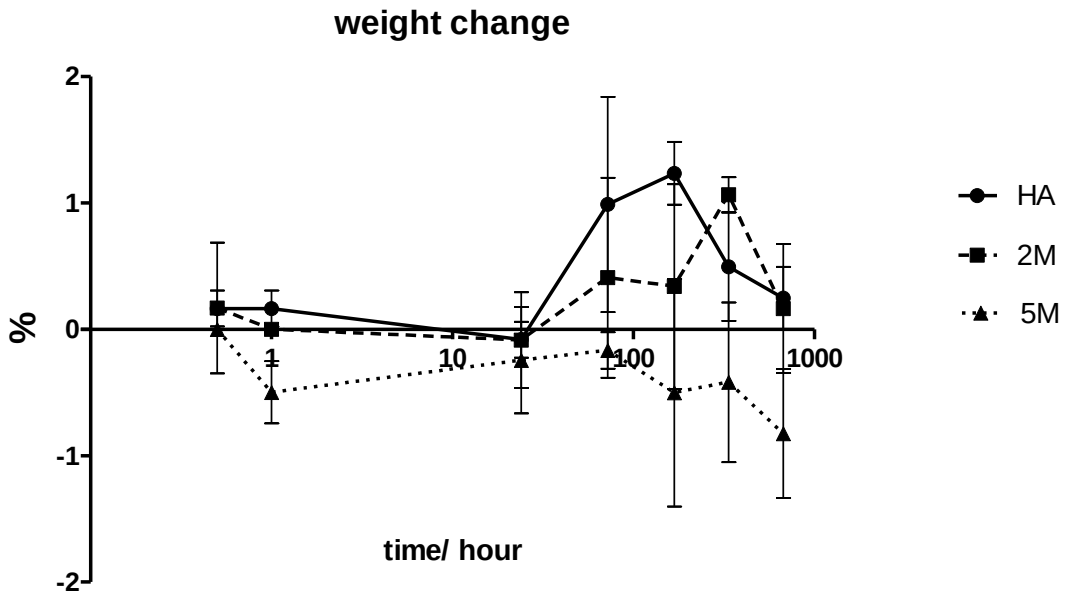

Figure 6.1 Weight change percentage

From previous unpublished results on release of calcium into the saline from HA and 2M samples, the HA samples didn't release much calcium into the saline the whole time and the release of calcium from 2M samples increases with time[87] (Figure 6.2). Therefore, we were expecting a weight loss in the infiltrated foams. But from the weight change result, this only seems to have been significant for the 5M samples. The reason for this trend becomes clearer when the surface of the foams were inspected by SEM and micro-CT.

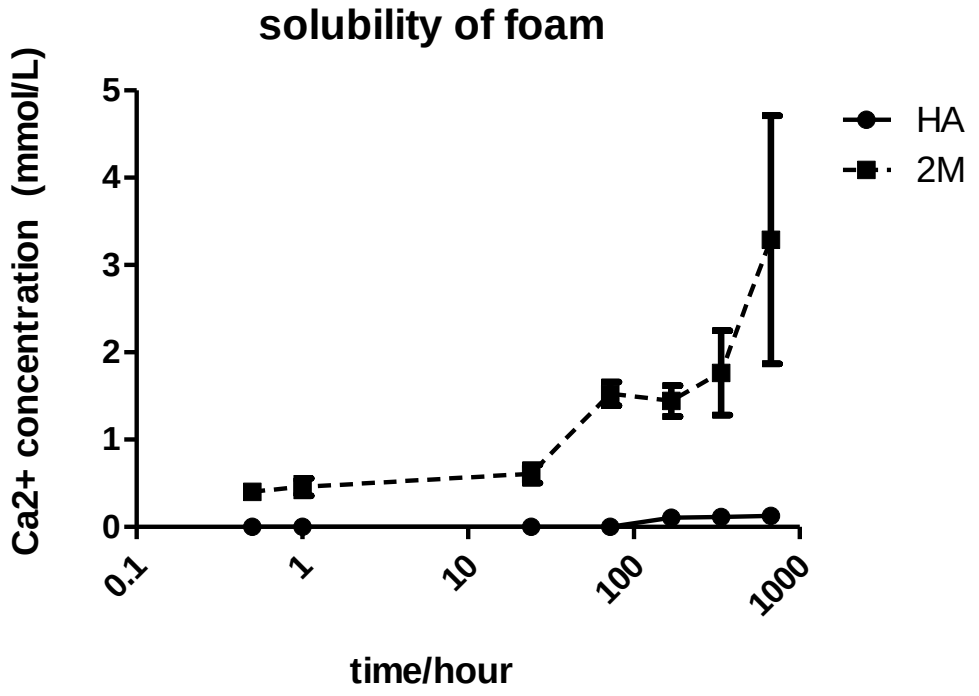

Figure 6.2 Ca^{+} content in the saline after solubility test[87]

6.2 SEM OBSERVATION

After infiltration and sintering, the introduced calcium might exist in the form of CaO or $Ca(OH)_2$. $CaCO_3$ also has a possibility of existing because of the reaction between $Ca(OH)_2$ and CO_2 in the air. All these phases will be termed as Ca rich phase relative to HA in the following discussion.

Figure 6.3 showed that all three sample conditions (HA, 2M and 5M) initially have smooth surface with a relatively low density of pores. As shown in the images, it is obvious that the density of pore of 5M samples is higher than that of 2M samples and pure HA. It indicates that the infiltration process might slightly increase the porosity of foams.

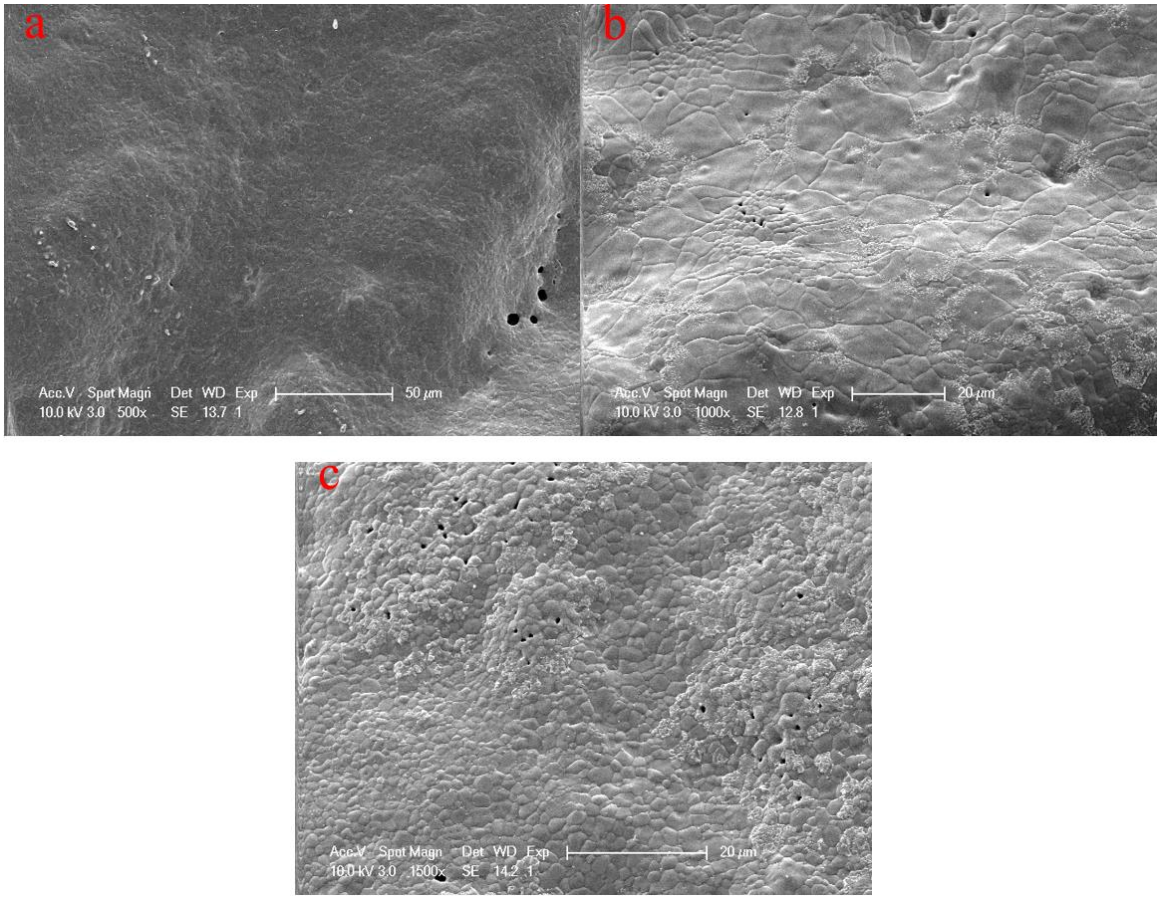

Figure 6.3 SEM images of surface of foams before solubility test (a) HA foam, (b) 2M foam, (c) 5M foam

After 1 hour of immersion (Figure 6.4), there is no distinct change in pure HA samples and no damage can be observed. For 2M samples, some damage can be observed. For 5M samples, there is some more defects and damage on the surface.

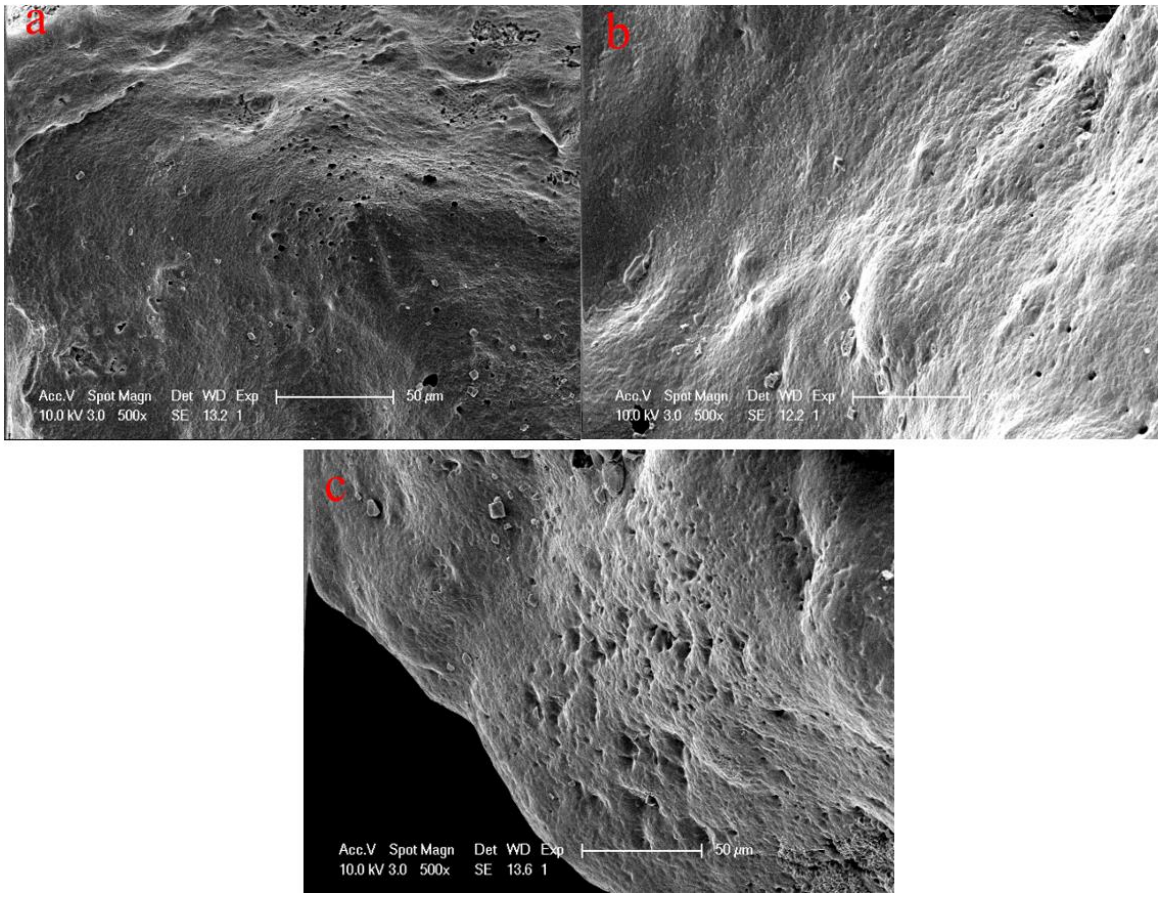

Figure 6.4 SEM images of surface of foams after 1 hour of immersion in TBS (a) HA foams, (b) 2M foams, (c) 5M foams

After 1 day of immersion (Figure 6.5), there is still no distinct change in pure HA foams. But for 2M samples, there is a large amount of needle-shaped phase (thought to be amorphous calcium phosphate precipitates[85]) on the surface and a relatively higher density of pitting on other place. For 5M samples, there are also many small defects on the edge of the frame. There is clearly more damage on the infiltrated samples.

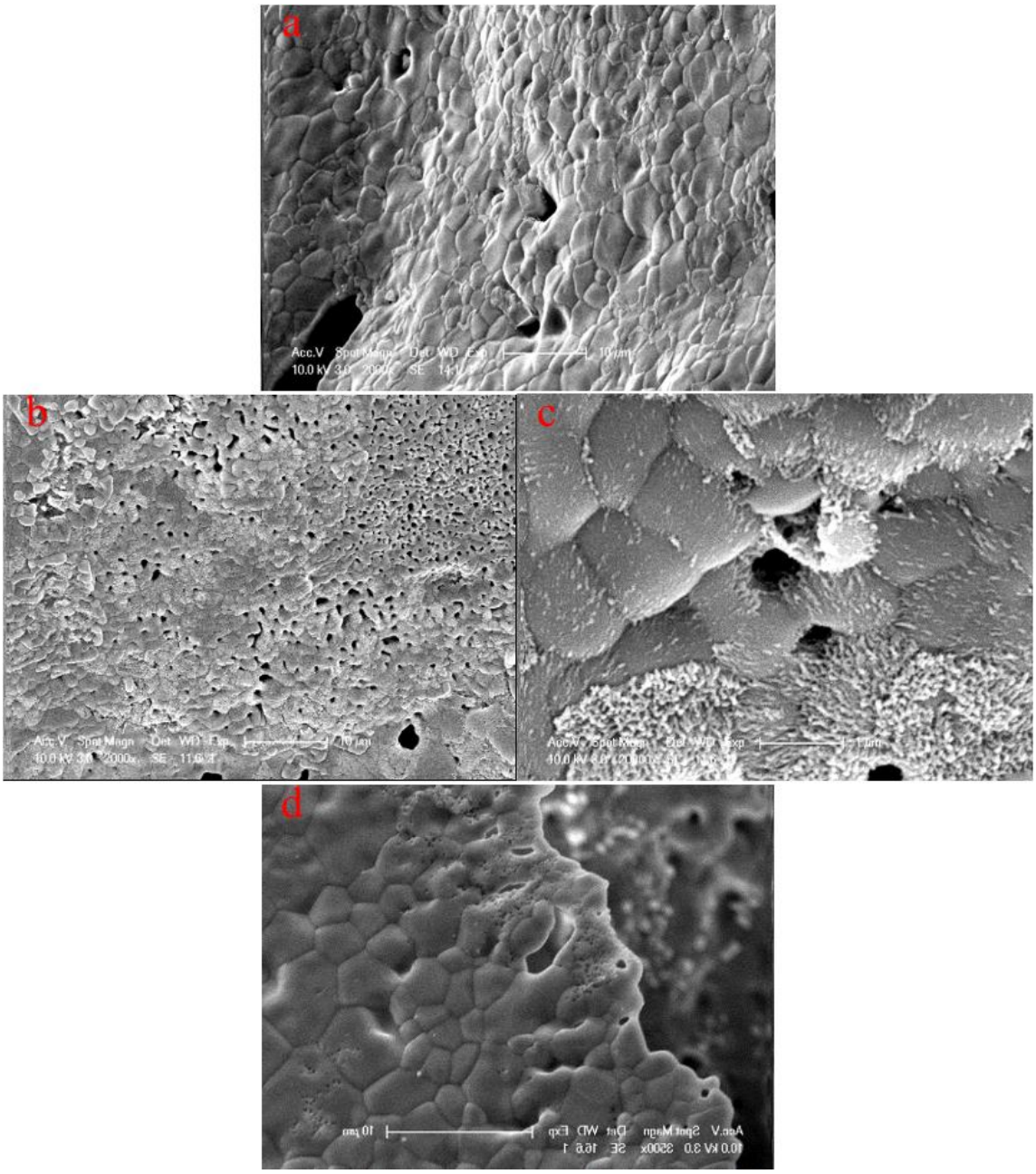

Figure 6.5 SEM images of surface of foams after 1 day of immersion in TBS (a) HA foams, (b) (c) 2M foams, (d) 5M foams

After 3 days of immersion (Figure 6.6), pure HA samples still have a smooth surface while some precipitation of the needle-shaped phase has occurred widely over the surface of 2M samples. For 5M samples, only a little amorphous precipitation can be found on the surface and the depth of pitting is greater than that in Figure 6.6 (d).

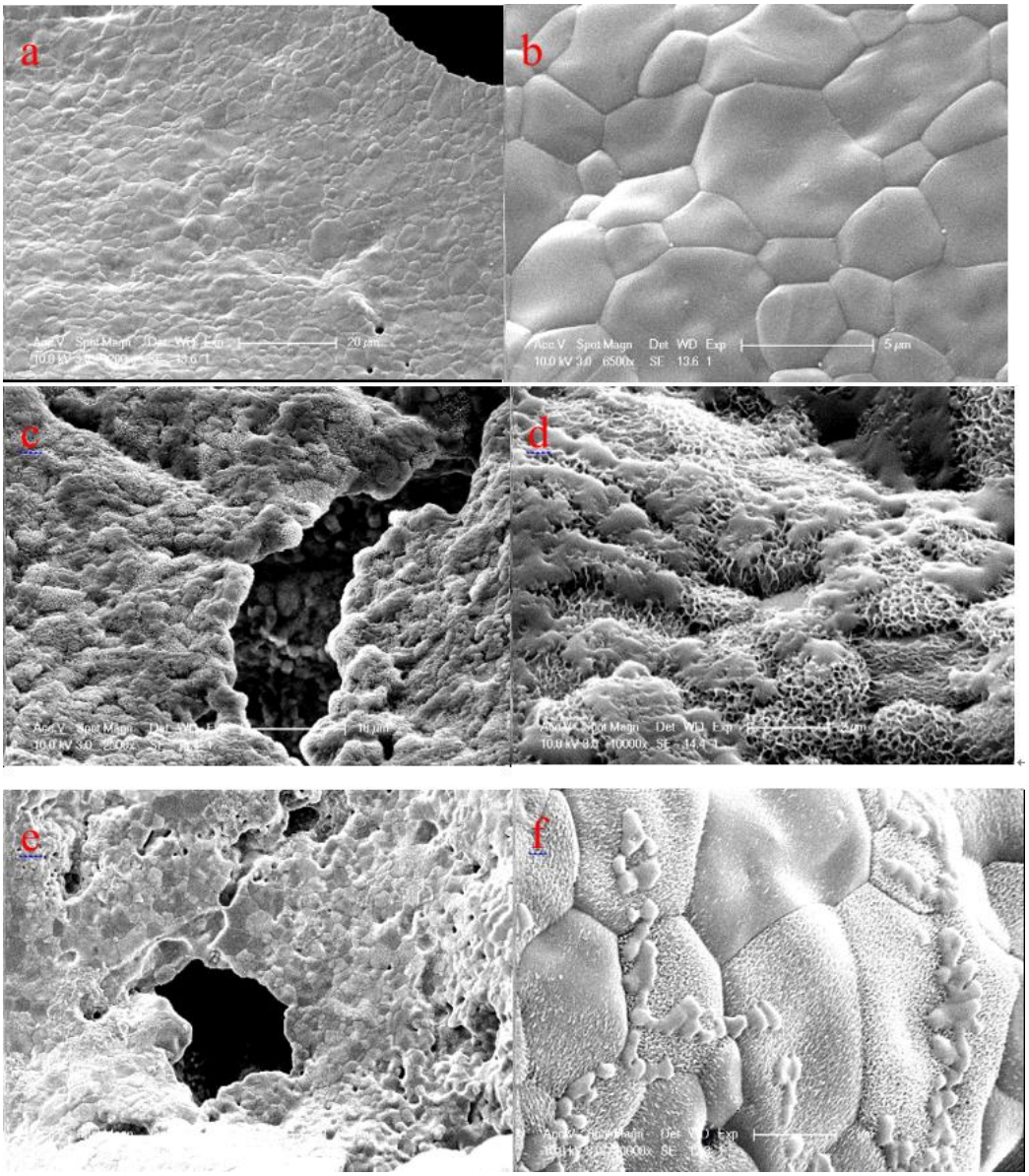

Figure 6.6 SEM images of surface of foams after 3 days of immersion in TBS (a) (b) HA foams, (c) (d) 2M foams, (e) (f) 5M foams

After 1 week (Figure 6.7), there is no change in pure HA and 2M samples relative to the 3 day time point. But the defects and pitting in 5M samples appear to even deeper.

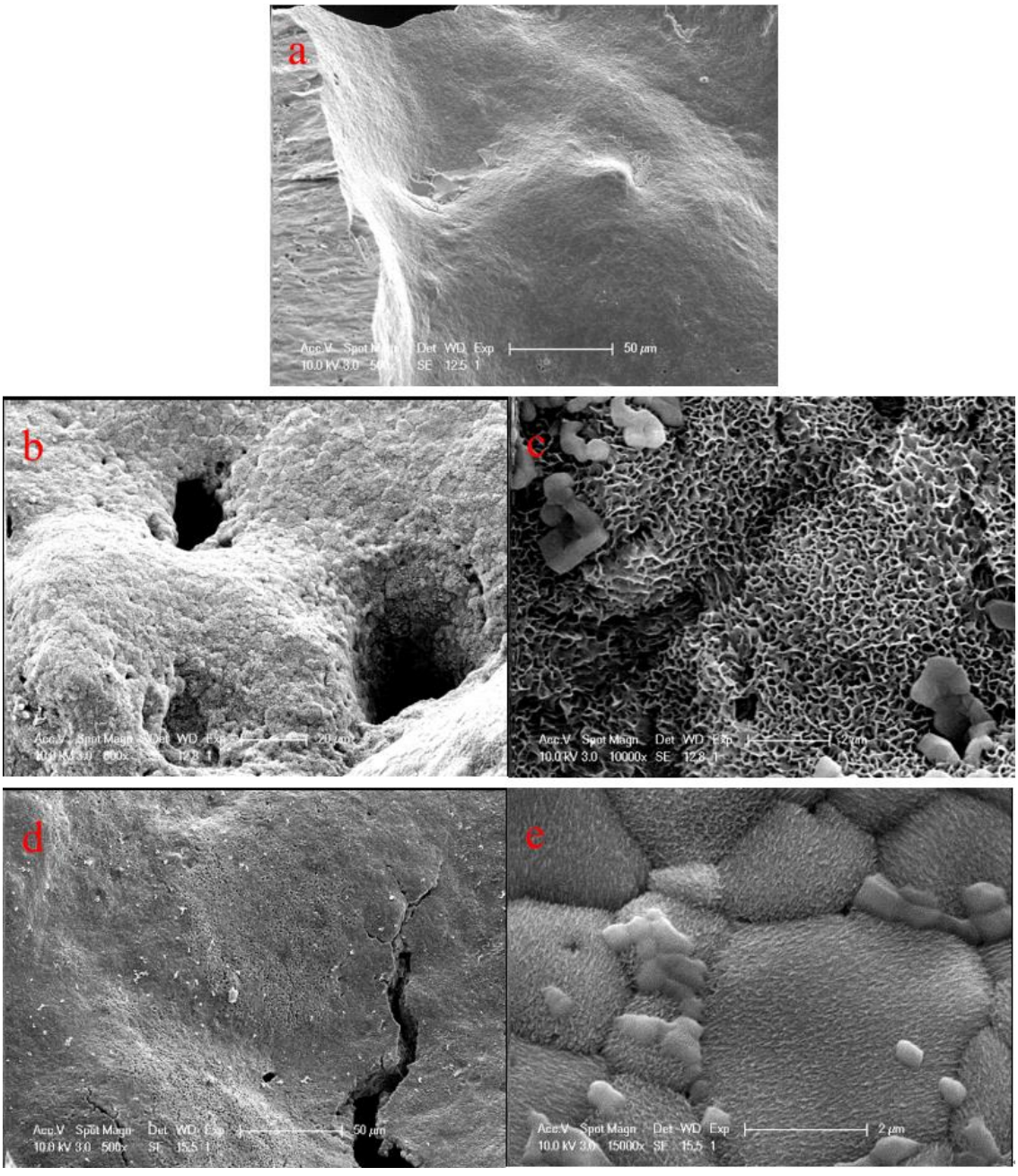

Figure 6.7 SEM images of surface of foams after 1 week of immersion in TBS (a) HA foams, (b) (c) 2M foams, (d) (e) 5M foams

After 4 weeks (Figure 6.8), some crystal precipitates was found on certain locations of the surface, this may be responsible for the small weight gain in the HA during the immersion in saline. The 2M foams show pits but also extensive precipitation. In contrast deeper pitting and more damage can be observed on the 5M samples.

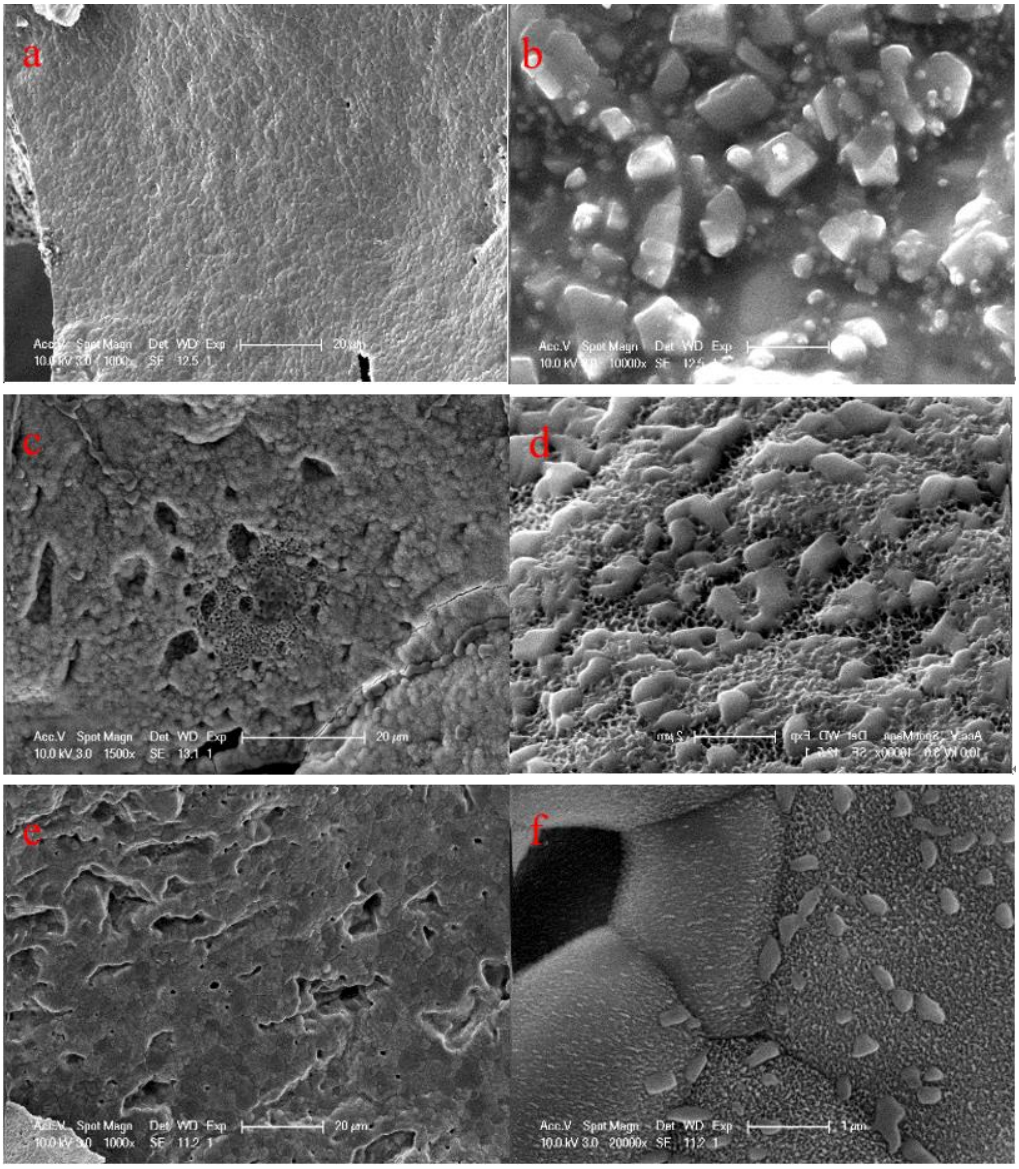

Figure 6.8 SEM images of surface of foams after 4 weeks of immersion in TBS (a) (b) HA foams, (c) (d) 2M foams, (e) (f) 5M foams

Summary: (i) The SEM observation appear to be in accordance with the weight change results. The reason for the weight gain of pure HA foams may because of the crystals generated from drying the saline during the test. (ii) 2M samples show surface precipitation and it increases with time. (iii) 5M samples show deeper pitting and more damage with time and few precipitates.

And from previous unpublished XRD result of the 2M samples (Figure 6.9), the presence of minor amounts of crystalline phases $CaCO_3$ that have been readily detected[8787].

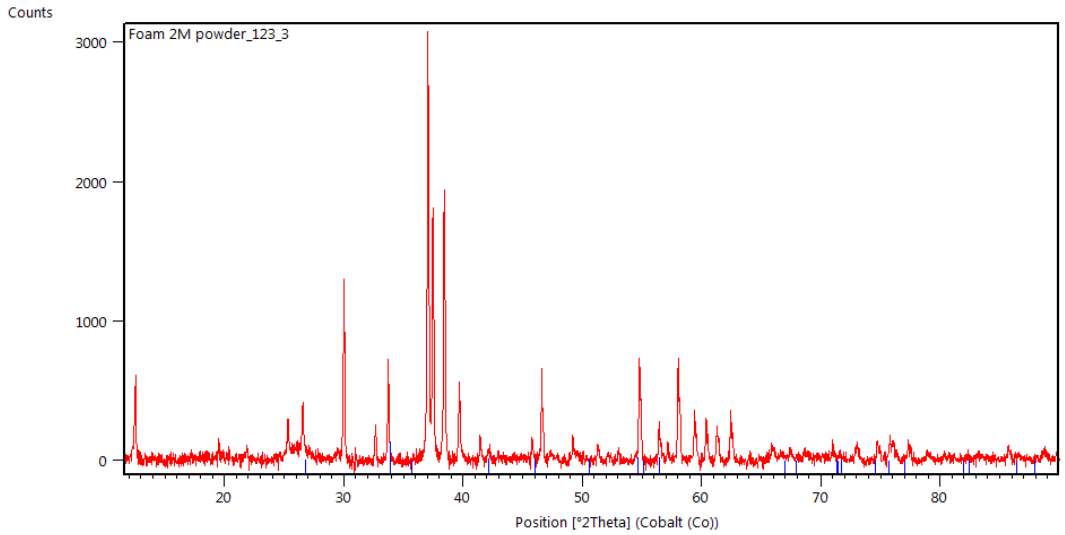

Figure 6.9 X-ray diffraction patterns of powder of 2M samples[87]

6.3 MICRO-CT

From the Micro-CT images, some properties, such as porosity, surface area, volume of foams, numbers of close pores and pore size distribution, can be calculated by the analysis program. But

due to the very large size of the pores relative to the size of the sample and the very high pore volume fraction it was not possible to close many of the pore sections from the slices for analysis of the pore size distribution and so this was not presented. Only the closed pores in the struts of the foam were analyzed.

Figure 6.10 shows the porosity of samples before and after the solubility test (4 weeks, 2 weeks, 1 week and 3days). From the figure, there is no significant trend can be observed and all the samples have porosities between 85% and 95%.

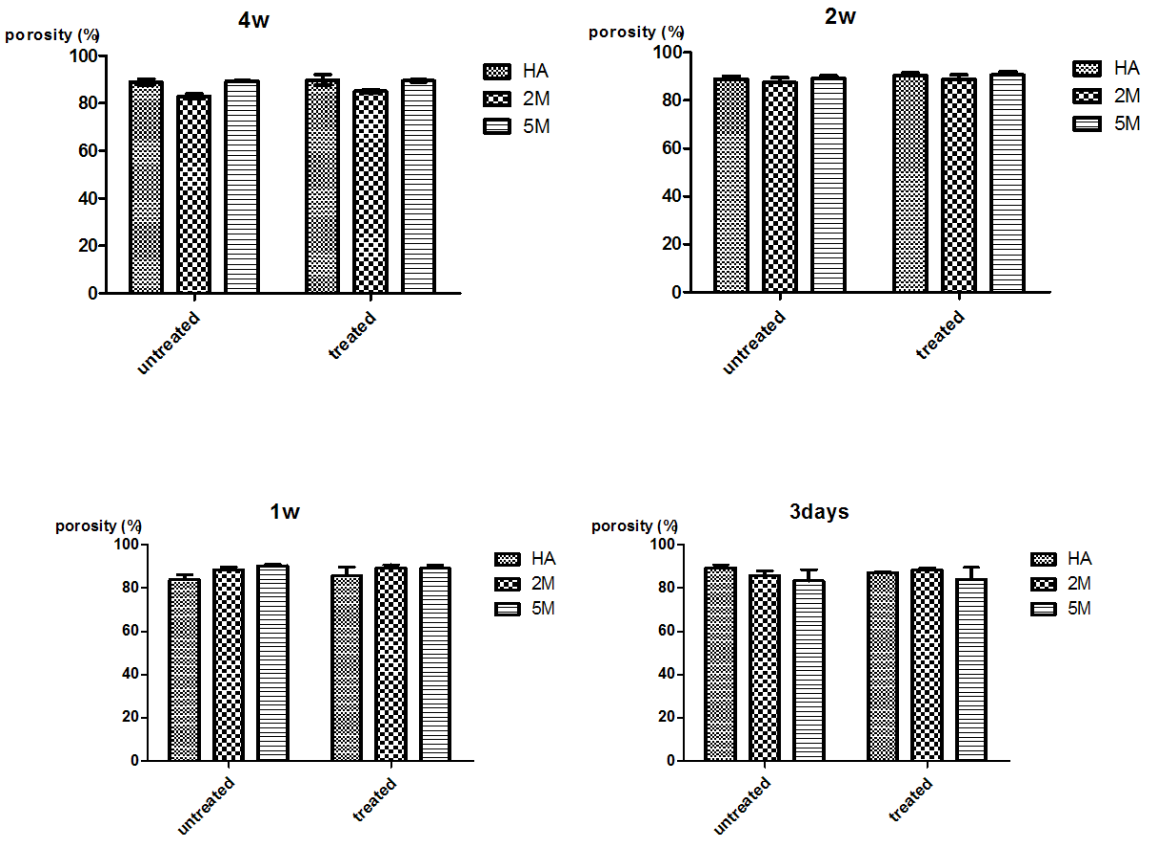

Figure 6.10 Porosity of samples before and after solubility test

Figure 6.11 and Figure 6.12 show the surface and porosity change percentage, respectively. The surface change tendency of HA and 5M samples are both similar to the porosity change. These changes don't show clear trends because of the variability of samples. Fig. Figure 6.12 suggests some increase in porosity for many samples that could be associated with some fragmentation. And it is apparent that the changes occurring on immersion such as the surface precipitation and the pitting occur at a too high magnification to affect the micro-CT results.

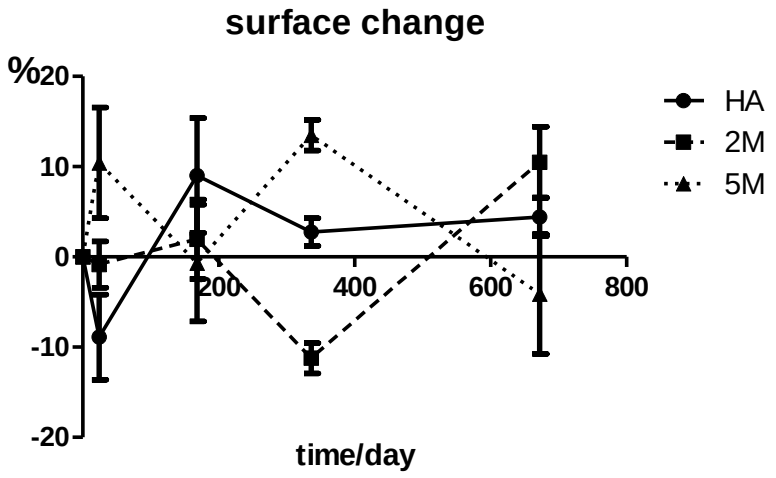

Figure 6.11 Surface change percentage of pure HA, 2M and 5M samples

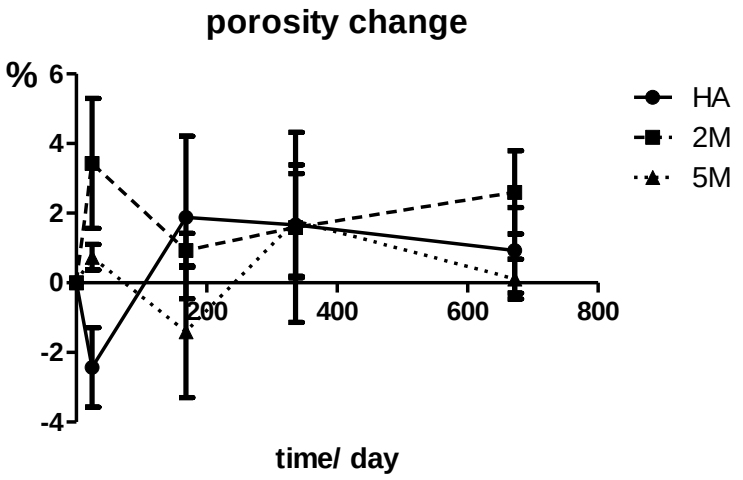

Figure 6.12 Porosity change percent of pure HA, 2M and 5M samples

During the immersion, the numbers of closed pores in 2M and 5M samples were expected to decrease with time due to the fragmentation. But as showed in Figure 6.13, the numbers of closed pores changed irregularly.

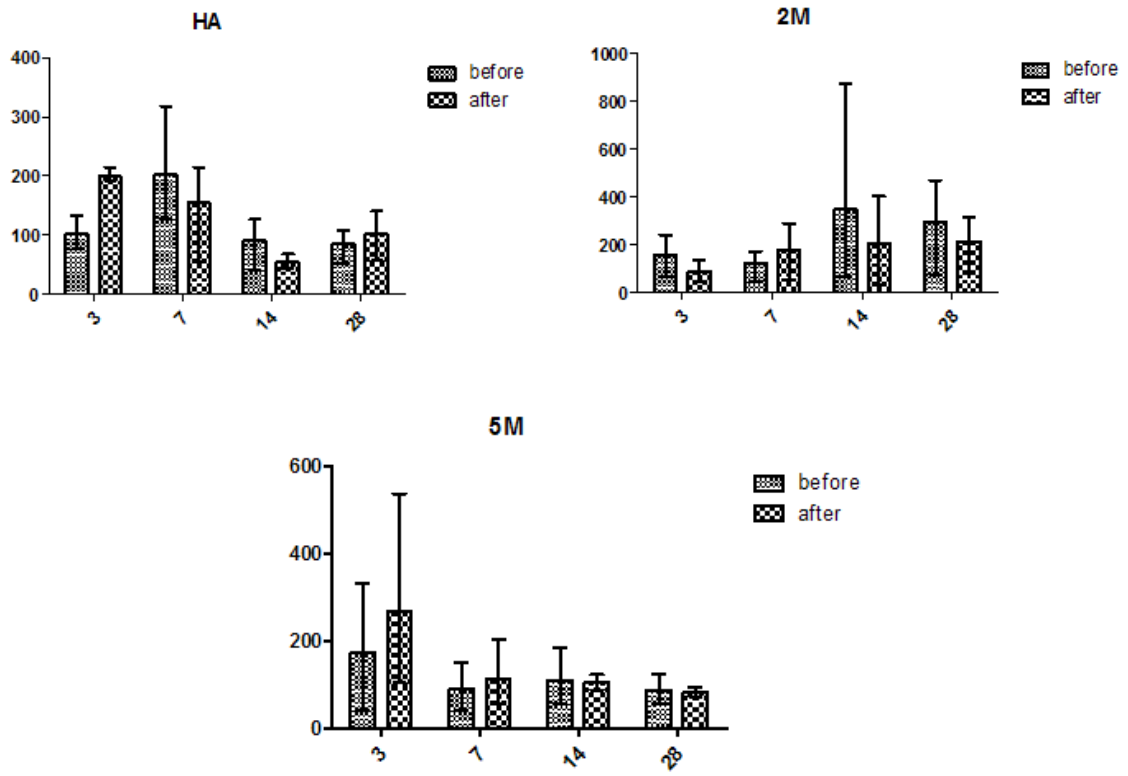

Figure 6.13 Number of closed pores in samples before and after the solubility test

Figure 6.14 shows the images of samples before and after the 4 weeks solubility test on approximate the same slice. These images show the microstructure clearly, we can observe the large pores that create large pore sections intersecting with the frame and cannot be closed and the small pores in the solid struts that are usually closed sections. But the problem of the comparison is when the sample was placed on the mount, the central axis of the sample was not perpendicular with the horizontal plane and the angle between the axis and the horizontal plane before and after the solubility test may not be the same. So the comparison of the cross sections can just be qualitative.

From Figure 6.14, there isn't much difference for all samples before and after the solubility test. It indicates that the minor difference observed in SEM images can't be showed in

micro-CT comparisons. And most important of all, there is no clear evidence of fragmentation can be observed.

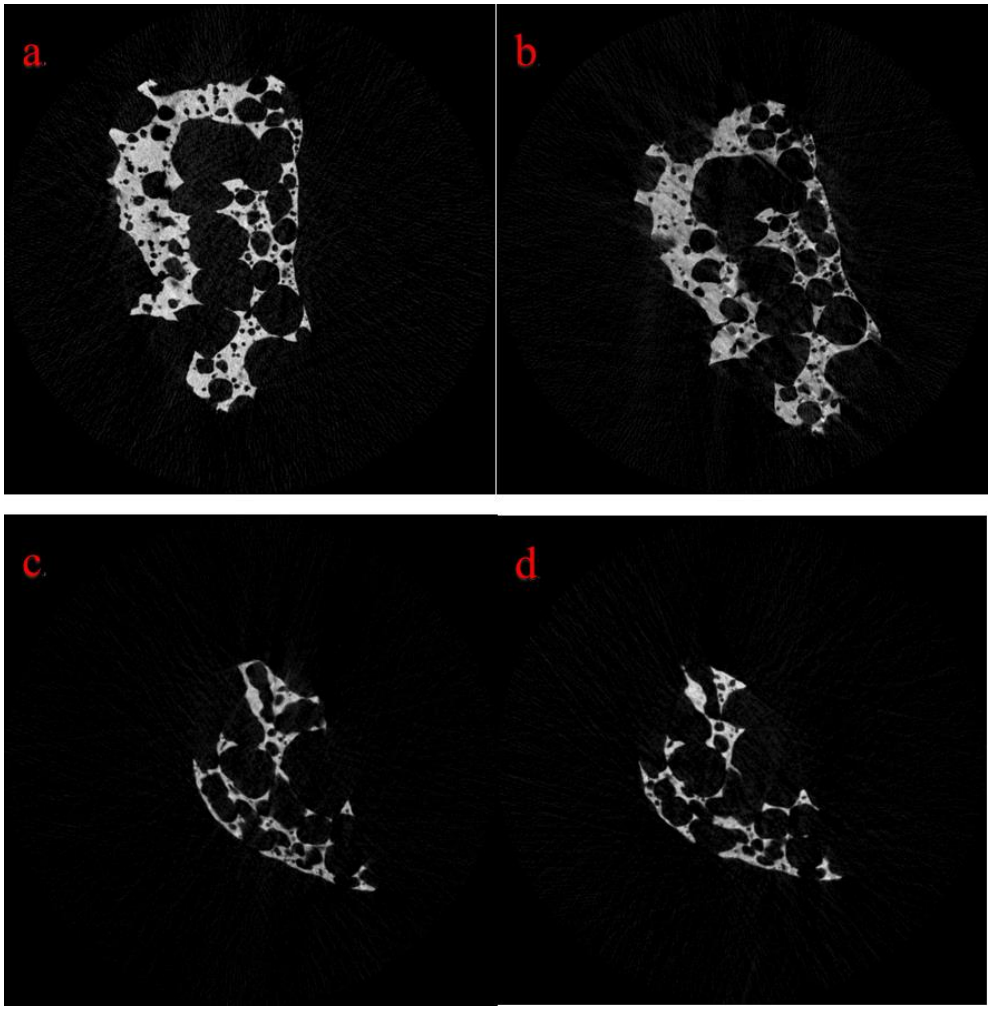

Figure 6.14 Cross section images of samples before and after the 4 weeks solubility test (a) (b)2M sample, (c) (d) 5M samples

7.0 CONCLUSION

1. A highly porous, approximately 90% pore space, calcium rich HA was fabricated by infiltrating calcium salt solution into HA foam that had been fabricated by an emulsion direct foaming method. The infiltration and sintering process produce HA with minor phases including $CaCO_3$.
2. The HA foam infiltrated with 5mol/L Ca^+ was the only sample that showed a weight loss and significant damage during the immersion in saline.
3. The 2M samples showed a lot of surface precipitation with some damage and no significant weight loss.
4. There is no evidence of large scale fragmentation of the foams during immersion for any of the samples studied.

8.0 FUTURE WORK

1. To reduce the effect of the variety of foam samples, larger and more samples should be used to repeat the solubility tests for each condition in the solubility test.
2. Comparison of micro-CT experiments should be conducted on the same sample in interrupted immersion experiments. This would avoid the problems with sample variability.
3. Foams should be tested with higher fractions of the calcium rich phases or tetracalcium phosphate by further increasing the calcium to phosphorous ratio in the powder used to make the foams.

BIBLIOGRAPHY

1 T.A. Einhorn, 'Enhancement of fracture-healing', J. Bone Joint Surg. Am., 77: 940–956, (1995)

2 Jeffrey D Hosenpud, Leah E Bennett, Berkeley M Keck, Mark M Boucek, et al, 'The registry of the international society for heart and lung transplantation: eighteenth official report—2001', The Journal of Heart and Lung Transplantation, 20(8) : 805–815 (2001)

3 Gahrton G, Björkstrand B, 'Progress in haematopoietic stem cell transplantation for multiple myeloma'. J Intern Med, 248 (3): 185–201. (2000).

4 Gratwohl, A., H. Baldomero, M. Gratwohl, M. Aljurf, L. F. Bouzas, M. Horowitz, Y. Kodera, et al. "Quantitative and Qualitative Differences in Use and Trends of Hematopoietic Stem Cell Transplantation: A Global Observational Study." Haematologica 98, no. 8 (August 1, 2013): 1282–90. doi:10.3324/haematol.2012.076349.

5 Shlomchik, Warren D. "Graft-versus-Host Disease." Nature Reviews Immunology 7, no. 5 (May 2007): 340–52. doi:10.1038/nri2000.

6 Remes, Kari, and Allan Rajamäki. "Autologous Stem Cell Transplantations." Annals of Medicine 28, no. 2 (January 1996): 79–82. doi:10.3109/07853899609092929.

7 Glotzbach, Jason P., Victor W. Wong, Geoffrey C. Gurtner, and Michael T. Longaker. "Regenerative Medicine." Current problems in surgery 48, no. 3 (march 2011): 148–212. Doi:10.1067/j.cpsurg.2010.11.002.

8 Science And Technology Committee Regenerative Medicine Report ,ordered to be printed 11 june 2013 and published 1 july 2013, published by the authority of the house of lords london : the stationery office limited

9 "Cell Therapy". American cancer society. 1 november 2008. Retrieved 15 september 2013.

10 Lefrère, J.-J.; Berche, P. (2010). "La Thérapeutique Du Docteur Brown-Séquard". Annales d'endocrinologie 71 (2): 69–75.doi:10.1016/j.ando.2010.01.003.

11 Starzl, Te (2000). "History of Clinical Transplantation". World journal of surgery 24(7): 759–82. Doi:10.1007/s002680010124.pmc 3091383. Pmid 10833242.

12 Handel M, 45S5-Bioglass(®)-based 3D-scaffolds seeded with human adipose tissue-derived stem cells induce in vivo vascularization in the CAM angiogenesis assay. Department Of Hygiene, Environment And Medicine, Hohenstein Institutes, Boennigheim, Germany.

13 Hing, Karin A. "Bioceramic Bone Graft Substitutes: Influence Of Porosity And Chemistry." International journal of applied ceramic technology 2, no. 3 (2005): 184–99.

14 Development of Biodegradable Porous Scaffolds for Tissue Engineering Guoping Chen A,), Takashi Ushida A,B, Tetsuya Tateishi A,B materials science and engineering c 17 2001 63–69

15 Martin I. et al, "Method for Quantitative Analysis of Glycosaminoglycan Distribution in Cultured Natural and Engineered Cartilage," (1999), Ann. Biomed. Eng., 27, 656-662.

16 Mc Dowell C.L.and Papoutsakis E.T.,(1998), "Increased Agitation Intensity Increases CD 13 Receptor surface Content and mRNA levels and Alters the Metabolism of HL60 Cells Cultured in Stirred tank Bioreactors," Biotechnol. Bioeng. 60, 239-250.

17 Lui Y. , Lui T., Fan X., Ma X., Cui.Z., "Ex-Vivo Expansion of Hhematopoietic Stem Cells Derived from Umbilical Cord Blood in Rotating Wall Vessel., (2006), J. Biotechno., 124, 592-601.

18 Fok E.Y. L.and Zandstra P.W. ,(2005) "Shear-Controlled Single-Step Mouse Embryonic Stem Cell Expansion and Embryoid Body Differentiation," Stem Cell, 23, 1333-1342.

19 Chen X., Xu H., Wan C., McCaigue M. and Li G., (2006) "Bioreactor Expansion of Human Adult Bone Marrow-Derived Mesenchymal Stem Cells," Stem Cell, 24, 2052-2059.

20 Marks Jr Sc, Odgren Pr. Structure and Development of The Skeleton. In: Bilezikian Jp, Raisz Lg, Rodan Ga, Editors. Principles of Bone Biology. 2nd Ed. San Diego: Academic Press; 2002. P. 3–15.

21 "Osteon," Encyclopædia Britannica Online (2009); Retrieved 23 June 2009.

22 http://en.wikipedia.org/wiki/Bone_marrow#cite_ref-1

23 Morrison, J.; Judith Kimble. 1) Asymmetric and symmetric stem-cell divisions in development and cancer.

24 Vunjak-Novakovic, G.; Tandon, N.; Godier, A.; Maidhof, R.; Marsano, A.; Martens, T. P.; Radisic, M., "Challenges In Cardiac Tissue Engineering". Tissue Engineering Part B: Reviews 16 (2): 169. (2010).

25 Domen, Amy Wagers And Irving L. Weissman “Regenerative Medicine” 2006 Terese Winslow

26 Pavletic Sz, Khouri If, Haagenson M, Et Al. "Unrelated Donor Marrow Transplantation For B-Cell Chronic Lymphocytic Leukemia After Using Myeloablative Conditioning: Results From The Center For International Blood And Marrow Transplant Research". J. Clin. Oncol. 23 (24): 5788–94.(2005)

27 Canellos, George (1997). "The Role Of Salvage Therapy In Malignant Lymphomas". The Oncologist2 (3): 181–183.

28 Bruno B, Rotta M, Patriarca F, et al. (2007). "A comparison of allografting with autografting for newly diagnosed myeloma". N. Engl. J. Med. 356(11): 1110–20. doi:10.1056/NEJMoa065464.PMID 17360989.

29 Gale Encyclopedia of Medicine. S.V. "Human Leukocyte Antigen Test." Retrieved December 7 2014

30 Immunobiology of Allogeneic Hematopoietic Stem Cell Transplantation Annual Review Of Immunology Vol. 25: 139-170 (Volume Publication Date April 2007) First Published Online As A Review In Advance On November 27, 2006 Doi: 10.1146/Annurev.Immunol.25.022106.141606 Lisbeth A. Welniak,1 Bruce R. Blazar,2,* And William J. Murphy1,*1department Of Microbiology And Immunology, University Of Nevada, Reno, Nevada 89557;

31 Russell N, Bessell E, Stainer C, Haynes A, Das-Gupta E, Byrne J (2000). "Allogenic haemopoietic stem cell transplantation for multiple myeloma or plasma cell leukaemia using fractionated total body radiation and high-dose melphalan conditioning".Acta Oncol 39 (7): 837–41.doi:10.1080/028418600750063596. PMID 11145442.

32 Nivison-Smith I, Bradstock KF, Dodds AJ, Hawkins PA, Szer J (2005). "Haemopoietic stem cell transplantation in Australia and New Zealand, 1992-2001: progress report from the Australasian Bone Marrow Transplant Recipient Registry". Intern Med J35 (1): 18–27. doi:10.1111/j.1445-5994.2004.00704.x. PMID 15667464.

33 Venkat, Chaya (July 19, 2005). "The Only Real Cure Out There, for Now ". CLL Topics, Inc.

34 https://hydroxyapatite.wikispaces.com/

35 https://en.wikipedia.org/wiki/Hydroxylapatite

36 L.-H. He, O.C. Standard, T.T.Y. Huang, B.A. Latella, M.V. Swain, Acta Biomater. 4 (2008) 577–586.

37 M. Mazaheri, M. Haghighatzadeh, A.M. Zahedi, S.K. Sadrnezhaad, J. Alloys Compd. 471 (2009) 180–184.

38 Jarcho M, Salsbury R.L, Thomas M. B, and Doremus R. H. Synthesis and Fabrication of β-Tricalcium Phosphate Ceramics for Potential Prosthestic Applications. J. Mater. Sci. 14:142, 1979.

39 Young R.A, and Holcomb D.W. Variability of Hydroxyapatite Preparations. Calcif. Tissue Int. 34 Suppl 2:S17-S32, 1982.

40 Kato K, Aoki H, Tabata T, and Ogiso M. Biocompatability of Apatite Ceramics in Mandibles. Biomat. Med. Dev. Art. Org. 7:291, 1979.

41 Williams D.F. The Biocompatibility and Clinical Uses of Calcium Phosphate Ceramics. pp. 43-66 in Biocompatibility of Tissue Analogs, Vol.II. Edited by Williams D.F. 1985.

42 de Groot K, Klein C.P.A.T, Wolke J.G.C, and de Blieck-Hogervorst J. Chemistry of Calcium Phosphate Bioceramics. pp. 3-15 in Handbook of Bioactive Ceramics, Vol.II. Edited by Yamamuro T, Hench L.L, and Wilson J. 1990.

43 R.W. Nurse, J.H. Welch, W. Gutt, J. Chem. Soc. 1959 (1959) 1077–1083.

44 M.J. Buerger, 'Crystallographic aspects of phase transformations', R. Smoluchowski, J.E. Meyer, W.A. Weyl (Eds.): 183–211, Phase transformations in solids, John Wiley, New York (1951)

45 Yashima, Masatomo, Atsushi Sakai, Takashi Kamiyama, and Akinori Hoshikawa. "Crystal Structure Analysis of B-Tricalcium Phosphate Ca3(PO4)2 by Neutron Powder Diffraction." Journal of Solid State Chemistry 175, no. 2 (November 2003): 272–77. doi:10.1016/S0022-4596(03)00279-2.

46 J.C. Elliott, Structure and Chemistry of the Apatites and Other Calcium Orthophosphates, Elsevier, Amsterdam, The Netherlands, 1994.

47 M. Bohner, 'Calcium orthophosphates in medicine: from ceramics to calcium phosphate cements', Injury, 31 (Suppl. D) : 37–47,(2000).

48 S.V. Dorozhkin. Calcium orthophosphate cements for biomedical application. J Mater Sci, 43 (2008), pp. 3028–3057.

49 Shinya Nakamura, Takuya Matsumoto, Jun-Ichi Sasaki, Hiroshi Egusa, et al, 'Effect of Calcium Ion Concentrations on Osteogenic Differentiation and Hematopoietic Stem Cell Niche-Related Protein Expression in Osteoblasts', Tissue engineering: Part A,8(16):2467-2473,(2010).

50 M.T. Fulmer, I.C. Ison, C.R. Hankermayer, B.R. Constantz, J. Ross, Measurements of the solubilities and dissolution rates of several hydroxyapatite. Biomaterials 23, 751–755 (2002)

51 Yang, H. Y., I. Thompson, S. F. Yang, X. P. Chi, J. R. G. Evans, and R. J. Cook. "Dissolution Characteristics of Extrusion Freeformed Hydroxyapatite–tricalcium Phosphate Scaffolds." Journal of Materials Science: Materials in Medicine 19, no. 11 (November 2008): 3345–53. doi:10.1007/s10856-008-3473-7.

52 M.Bohner, ' Calcium orthophosphates in medicine: from ceramics to calcium phosphate cements', J.Care Injured, 31(2000)

53 N. OzguÈr Engin and A. CuÈneyt Tas "Manufacture of Macroporous Calcium Hydroxyapatite Bioceramics" Journal of the European Ceramic Society 19 (1999) 2569-2572

54 T. Ohji* and M. Fukushima "Macro-porous ceramics: processing and properties" International Materials Reviews 2012 VOL 57 NO 2 131

55 Ohgushi, H., Okumura, K. and Yoshikawa, T., Bone formation process in porous calcium carbonate and hydroxyapatite. J. Biomed. Mater. Res., 1992, 26, 885± 895

56 Passuti, N., Daculsi, G., Rogez, J. M., Martin, S. and Bainvel, J. V., Macroporous calcium phosphate ceramics performance in human spine fusion. Clin. Orthoped., 1989, 148, 169±176.

57 Klawiter, J. J., Bagwell, J. G., Weinstein, A. M., Sauer, B. W. and Pruitt, J. R., An evaluation of bone growth into porous high density polyethylene. J. Biomed. Mater. Res., 1976, 10, 311±321.

58 Wei G, Ma PX. Structure and properties of nano-hydroxyapatite/polymer composite scaffolds for bone tissue engineering. Biomaterials. 2004;25(19):4749–4757.

59 I. H. Arita, V. M. Castano, and D. S. Wilkinson, ''Synthesis and Processing of Hydroxyapatite Ceramic Tapes with Controlled Porosity,'' J. Mater. Sci.—Mater. Med., 6 [1] 19–23 (1995).

60 AR Studart, UT Gonzenbach, E Tervoort, et al,,' Processing Routes to Macroporous Ceramics: A Review', Journal of the American Ceramic Society, 89(6): 1771–1789, 2006

61 F. F. Lange and K. T. Miller, ''Open-Cell, Low-Density Ceramics Fabricated from Reticulated Polymer Substrates,'' Adv. Ceram. Mater., 2 [4] 827–31 (1987).

62 P. Sepulveda, ''Gelcasting Foams for Porous Ceramics,'' Am. Ceram. Soc. Bull., 76 [10] 61–5 (1997).

63 J. Saggio-Woyansky, C. E. Scott, and W. P. Minnear, ‘‘Processing of Porous Ceramics,’’ Am. Ceram. Soc. Bull., 71 [11] 1674–82 (1992).

64 P. Colombo, E. Bernardo, and L. Biasetto, ‘‘Novel Microcellular Ceramics from a Silicone Resin,’’ J. Am. Ceram. Soc., 87 [1] 152–4 (2004).

65 O. Lyckfeldt and J. M. F. Ferreira, ‘‘Processing of Porous Ceramics by Starch Consolidation,’’ J. Eur. Ceram. Soc., 18 [2] 131–40 (1998).

66 T. J. Fitzgerald, V. J. Michaud, and A. Mortensen, ‘‘Processing of Microcellular Sic Foams. 2. Ceramic Foam Production,’’ J. Mater. Sci., 30 [4] 1037–45 (1995).

67 P. Colombo, E. Bernardo, and L. Biasetto, ‘‘Novel Microcellular Ceramics from a Silicone Resin,’’ J. Am. Ceram. Soc., 87 [1] 152–4 (2004).

68 Y. Hotta, P. C. A. Alberius, and L. Bergstrom, ‘‘Coated Polystyrene Particles as Templates for Ordered Macroporous Silica Structures with Controlled Wall Thickness,’’ J. Mater. Chem., 13 [3] 496–501 (2003).

69 T. Fukasawa, M. Ando, T. Ohji, and S. Kanzaki, ‘‘Synthesis of Porous Ceramics with Complex PoreStructure by Freeze–Dry Processing,’’ J.Am. Ceram. Soc., 84 [1] 230–2 (2001).

70 I. Akartuna, A. R. Studart, U. T. Gonzenbach, E. Tervoort, and L. J. Gauckler, ‘‘Porous Ceramics from Particle-Stabilized Emulsions,’’ Adv. Mater., (2006), in Preparation.

71 E. S. Toberer, J. C. Weaver, K. Ramesha, and R. Seshadri, ‘‘Macroporous Monoliths of Functional Perovskite Materials Through Assisted Metathesis,’’ Chem. Mater., 16 [11] 2194–200 (2004).

72 8H. Wang, I. Y. Sung, X. D. Li, and D. Kim, ‘‘Fabrication of Porous SiC Ceramics with Special Morphologies by Sacrificing Template Method,’’ J. Porous Mater., 11 [4] 265–71 (2004).

73 N. Miyagawa and N. Shinohara, ‘‘Fabrication of Porous Alumina Ceramics with Uni-Directionally-Arranged Continuous Pores Using a Magnetic Field,’’ J. Ceram. Soc. Jpn., 107 [7] 673–7 (1999).

74 U. T. Gonzenbach, A. R. Studart, E. Tervoort, and L. J. Gauckler, ‘‘Ultrastable particle-stabilized foams,’’ Angewandte Chemie—Int. Ed., (2006), in press. 154S. U. Pickering, ‘‘Emulsions,’’ J. Chem. Soc., 91, 2001–21 (1907).

75 "Sinter, v." Oxford English Dictionary Second Edition on CD-ROM (v. 4.0) © Oxford University Press 2009

76 Rahaman MN. Sintering of ceramics. Boca Raton: CRC Press; 2008.

77 Kleebe HJ, Bres EF, Bernache-Assollant D, Ziegler G. High-resolution electron microscopy and convergent beam electron diffraction of sintered undoped hydroxyapatite. J Am Ceram Soc 1997;80:37–44.

78 http://www.keramverband.de/brevier_engl/4/1/4_1_4.htm

79 S. J. Glass and D. J. Green, "Surface Modification of Ceramics by Partial Infiltration" Adv. Ceram. Mater., 2[2] 129-31(1987)

80 W. C. Tu and F. F. Lange. "Liquid Precursor Infiltration Processing of Powder Compacts: 1, Kinetic Studies and Microstructure Devolpment," J, Am, Ceram. Soc. 78 [12] 3277-82 (1995)

81 Marple, Basil Richard, and David J. Green. "Graded Compositions and Microstructures by Infiltration Processing." Journal of Materials Science 28, no. 17 (1993): 4637–43.

82 Lin, Yung-Jen, and Yi-Chi Chen. "Cyclic Infiltration of Porous Zirconia Preforms with a Liquid Solution of Mullite Precursor." Journal of the American Ceramic Society 84, no. 1 (January 2001): 71–78. doi:10.1111/j.1151-2916.2001.tb00610.x.

83 P. Honeyman-Colvin and F F.Lange, 'Infiltration of porous alumina bodies with solution precursors: strengthing cia compositional grading , grain size control , and transformation toughening' , J.Am.Ceram.Soc.,79(7):1810-1814,(1996)

84 Marple, Basil Richard, and David J. Green. "Graded Compositions and Microstructures by Infiltration Processing." Journal of Materials Science 28, no. 17 (1993): 4637–43.

85 Wang, Haibo, Jong-Kook Lee, Amr Moursi, and John J. Lannutti. "Ca/P Ratio Effects on the Degradation of Hydroxyapatite in Vitro." Journal of Biomedical Materials Research Part A 67, no. 2 (2003): 599–608.

86 Hoppe, Alexander, Nusret S. Güldal, and Aldo R. Boccaccini. "A Review of the Biological Response to Ionic Dissolution Products from Bioactive Glasses and Glass-Ceramics." Biomaterials 32, no. 11 (April 2011): 2757–74. doi:10.1016/j.biomaterials.2011.01.004.

87 Qinghao Zhang, unpublished article, department of materials science and engeering, University of Pitssburgh